To appear in the *Astronomical Journal*, July 1997.

Evidence for Cleared Regions in the Disks Around Pre–Main-Sequence Spectroscopic Binaries

Eric L. N. Jensen[1] and Robert D. Mathieu
Univ. of Wisconsin-Madison, Dept. of Astronomy,
475 N. Charter St., Madison, WI 53706.
Electronic mail: Eric.L.N.Jensen@asu.edu, mathieu@astro.wisc.edu.

ABSTRACT

Combining new infrared photometry with data in the literature, we have compiled spectral energy distributions (SEDs) from optical to millimeter wavelengths for four low-mass pre–main-sequence spectroscopic binaries ($a < 1$ AU) showing infrared excesses. Three of these binaries have small or no excess emission at $\lambda = 1$–$5\ \mu$m but large excess emission at longer wavelengths, suggesting cleared regions within circumbinary disks. The inferred sizes of these gaps or holes are consistent with theoretical predictions for dynamical clearing by stellar companions. In contrast, the binary AK Sco has a power-law SED with no evidence of reduced near-infrared emission. Nonetheless, a strong 9.8 μm silicate emission feature suggests the presence of optically thin dust, and the near-infrared emission can be produced by very small amounts ($\sim 10^{-9}\ M_\odot$) of material within a gap or hole. Thus a dynamically cleared region may exist in AK Sco but is not required by the data.

That three of these binaries (and several other short-period pre–main-sequence binaries) have near-infrared excesses indicative of hot material near the stars is significant given that circumstellar disk radii are limited to less than 0.06 AU (or several stellar radii). The spatial distribution of the near-infrared-emitting material may not be disk-like. Continued replenishment is necessary, perhaps from circumbinary disks.

Circumbinary disk masses around short-period pre–main-sequence binaries range from 0.06 $M_\odot$ to less than $10^{-4}\ M_\odot$. The larger disk masses are sufficient to substantially influence the binaries' orbital eccentricities during their pre–main-sequence lifetimes.

---

[1]Present address: Dept. of Physics and Astronomy, Arizona State University, P. O. Box 871504, Tempe, AZ 85287-1504.

Subject headings: stars: binaries: general — stars: pre–main-sequence — circumstellar matter

1. Introduction

Recent observations have revealed that a majority of young, low-mass stars are members of binary systems (Mathieu et al. 1989, Ghez et al. 1993, Leinert et al. 1993, Reipurth & Zinnecker 1993, Simon et al. 1995). Many young stars (including binary systems) are surrounded by gas and dust, probably in disks (e.g., Sargent 1996). Thus the interaction of a binary and an associated disk is a common process in early stellar evolution.

A young binary system may contain up to three distinct disks: circum*stellar* disks around one or both stars in the binary, with disk radii smaller than the binary's periastron separation, and a circum*binary* disk lying entirely outside the binary orbit. These disks are remnants of the star formation process and thus may provide clues about binary formation mechanisms. At the same time, disks influence the evolution of binary systems through mass flow and accretion and through dynamical interactions which may drive orbital evolution. The location and amount of disk material determine what types of planets the system might form and how quickly their orbits may evolve.

The theoretical expectations for the distribution of disk material in a binary system are clear, at least in broad terms. A binary system embedded in a disk should rapidly clear away material in the region near the binary orbit (e.g., Lin & Papaloizou 1993 and references therein); the size of the cleared region depends on the binary semi-major axis, mass ratio, and eccentricity, as well as on disk properties such as viscosity (Artymowicz & Lubow 1994). It has typically been assumed that the gaps are free of material and that the circumbinary disk and circumstellar disks evolve independently of each other once a gap has been cleared. In the absence of replenishment, continued accretion may exhaust circumstellar disks, leaving only the binary within a central hole in the circumbinary disk.

Observational evidence for binary-disk interactions comes from millimeter-wavelength observations, which provide a probe of the total disk mass in binary systems. Binaries with separations of 1–100 AU have substantially less disk material than wider binaries or single stars (Beckwith et al. 1990, hereinafter BSCG; Jensen et al. 1994, 1996a; Osterloh & Beckwith 1995). The *IRAS* 60 μm fluxes of these systems show that most binaries do have circumstellar disks, though neither the exact location of the material nor its surface density are well constrained (Jensen et al. 1996a).

The spatial distribution of disk material can be more directly determined by imaging, and indeed images of the disks around a few binaries have been made at millimeter and infrared wavelengths. GG Tau (projected separation 35 AU) is surrounded by an extended circumbinary disk with a central clearing (Dutrey et al. 1994, Roddier et al. 1996). In contrast, UZ Tau W (projected separation 50 AU) has no circumbinary disk, but substantial mass in one or two circumstellar disks (Jensen et al. 1996b). The marked differences in the disk morphologies of these two systems and the small number of binaries whose disks have been imaged at high resolution permit few general conclusions about disk structure in young binaries to be drawn.

Because the nearest star-forming regions lie at distances of 100–200 pc, direct imaging of disk material on size scales of a few AU is not possible with current instrumentation. Thus, the inner regions of disks, where accretion onto the stars occurs and where terrestrial planets may form, must be probed indirectly. One technique for doing so involves comparison of the relative strength of disk emission at different wavelengths. The temperature of disk material around a star is expected to decrease with radial distance from the star, whether the disk heating is dominated by the star or by accretion. The wavelength of the peak emission from a given disk annulus is a function of the temperature in the annulus and therefore of distance from the star. Removing material at certain radial distances from the central star(s) thus predominantly removes emission at certain wavelengths. The emission deficit at these wavelengths appears as a “dip”, or deviation from a smooth decrease, in the emitted spectral energy distribution (SED), thereby allowing detection of disk gaps or central holes using spatially unresolved photometric data.

This technique of detailed SED modeling has been applied to a few binary systems to infer the presence of gaps in their disks (GW Ori, Mathieu et al. 1991, 1995; DF Tau, Marsh & Mahoney 1993). In addition, Simon & Prato (1995) used $K - N$ colors to make a systematic search for evidence of disk clearing in young binaries. They found that inner disk clearing (as measured by $K - N$) is not more common in binaries than in single stars. However, their binary sample was dominated by systems with projected separations greater than a few AU, and as they point out, binaries with smaller separations may be more likely to clear the parts of disks that emit strongly at near- and mid-infrared wavelengths.

In this work, we present a systematic study of the disks in four young binaries with projected separations less than 1 AU. As discussed in Sec. 2, we have made ground-based infrared observations of several binaries in order to compile well-sampled SEDs. We discuss our technique for modeling these SEDs in Sec. 3 and the model results in Sec. 4. We then discuss our conclusions about disk clearing and evolution in young binary systems in Sec. 5.

2. Sample Selection and Observations

We have drawn our targets from a parent sample of pre–main-sequence (PMS) binaries with disks (as judged by their detection by *IRAS* at 12 μm) and with separations less than 1 AU. This parent sample has been taken from the list of PMS binaries given by Mathieu (1994) plus three PMS spectroscopic binaries discovered later (V773 Tau, UZ Tau E, and DQ Tau; Welty 1995, Mathieu et al. 1996, 1997), and are listed in Table 1. Of these binaries, GW Ori, DQ Tau, and UZ Tau E already been modeled extensively (Mathieu et al. 1991, 1995; Mathieu et al. 1997; Jensen et al. 1996b). We include them in our discussion, but do no further modeling in this paper. The binaries W134 (Padgett & Stapelfeldt 1994) and V773 Tau were discovered to be binaries after our observations were complete; not enough photometric data are available to allow useful modeling and so they are not discussed further. The binaries 162814−2427, V4046 Sgr, 162819−2423S, and AK Sco comprise the target binaries observed and analyzed here.

We do not include wider binaries in our sample to be modeled, but during the course of our observing program we did make some observations of wider binaries for other purposes. In the interest of completeness the data for the wider binaries are presented here as well.

We made near- and mid-infrared photometric observations at the NASA Infrared Telescope Facility (IRTF) on 8 and 9 June 1992 and 17 and 19 June 1993, and at the United Kingdom Infrared Telescope (UKIRT) on 26 May 1993.[2] The IRTF observations used a 3-mm aperture which corresponds to $5\farcs85$ projected on the sky. The 1992 IRTF observations used a chop throw of $20''$ north-south, while the 1993 IRTF observations used a chop throw of $15''$ north-south. The UKIRT observations used apertures of $5\farcs0$ and $7\farcs8$ and a chop throw of $30''$ east-west.

The photometric observations were calibrated using frequent observations of standard stars throughout the night. Magnitudes for the standard stars at $JHKL'MNQ$ were taken from Tokunaga (1988); magnitudes for standard stars in the 7.8–12.5 μm narrow-band filters were taken from Tokunaga et al. (1986) and Hanner et al. (1984). For each filter, the atmospheric extinction and the offset between the instrumental and standard magnitude systems were determined from a linear fit to the difference between instrumental and known standard-star magnitudes as a function of airmass. In some cases, there was a change in the sky conditions during the night and a single extinction curve did not provide a good fit to

[2]The Infrared Telescope Facility is operated by the University of Hawaii under contract to the National Aeronautics and Space Administration. The United Kingdom Infrared Telescope is operated by the Royal Observatory, Edinburgh, on behalf of the Particle Physics and Astronomy Research Council of the United Kingdom.

the entire night's data. In these cases, the night was divided into two parts and each was calibrated separately.

For the IRTF M, N, Q, and narrow-band 7.8–12.5 μm filters, the observations of α Boo (K1 III) and α Sco (M1.5 I) yielded measured magnitudes when reduced using α Lyr that were 0.03–0.09 magnitudes brighter than their catalog magnitudes. Since late-type stars in general (and α Sco in particular) are known to vary at these wavelengths (Tokunaga 1988), we adopted α Lyr (A0 V) as our primary standard for the M, N, Q, and narrow-band filters. Both α Boo and α Sco showed the same atmospheric extinction curve as α Lyr (though different zero points given their nominal catalog magnitudes), indicating that conditions were stable across the sky. Thus we used α Boo and α Sco as secondary standards and adopted slightly brighter catalog magnitudes for them to bring them into agreement with the α Lyr observations. The reduced magnitudes for the target PMS binaries are given in Tables 2–4.

2.1. The Observed Spectral Energy Distributions

For each of the four binaries we derived an SED from all available optical, infrared, submillimeter, and millimeter photometry available from our own observations and from the literature. The SEDs are shown in Figs. 1–4. Also shown as dashed curves are the SEDs of model stellar photospheres appropriate for each binary (Sec. 3.2).

Most of the systems modeled here are variable at optical and infrared wavelengths, as are most PMS stars (e.g., Cohen & Schwartz 1976, Herbst et al. 1994). At optical wavelengths ($UBVR_CI_C$) where multiple observations of a given system were available, we adopted the brightest observation available at each wavelength. In doing so we presume that the variability arises from cool stellar spots or variable circumstellar extinction (Herbst et al. 1994); thus adopting the brightest set of observations gives the best estimate of the actual photospheric flux.[3] At longer wavelengths, typically fewer measurements are available and the presence and origin of any variability are more uncertain. For these wavelengths we computed the mean brightness of the system for use in our model fitting. For each system we show the observed range of variability with error bars [Panel (a) of

---

[3]Some of the U and B flux may arise from boundary-layer emission (Herbst et al. 1994), so adopting the brightest measurement may emphasize the ultraviolet excess in some systems. We do not include boundary-layer emission in our modeling, nor do we use the U flux in determining the photospheric luminosity. If the boundary-layer emission is strong enough to contribute substantial B flux, this could in principle lead to an overestimate of the stellar luminosity.

Figs. 1–4]. In most cases our conclusions would be unchanged by adopting any of the values within the measured range of variability; we comment individually on systems in which variability might influence the conclusions.

Three of the four binaries (162814−2427, 162819−2423S, and V4046 Sgr) have SEDs that deviate greatly from the power-law slope expected from a continuous disk with a power-law temperature distribution (e.g., Adams et al. 1988). These SEDs show small or no emission excesses from 1–5 μm but large infrared excesses at $\lambda \geq 10$ μm. The relative lack of near-infrared emission from these binaries suggests a deficit of hot disk material, as would be expected if inner disk regions had been cleared by the binaries. On the other hand, the SED of AK Sco resembles the power-law distribution of a continuous disk.

3. Modeling Disk Emission

Motivated by the theoretical prediction that binaries clear regions in associated disks, we now examine the emission from these binaries in more detail. In particular, we develop models for the SEDs of disks having cleared gaps or holes and compare them to the observed SEDs. In this section, we present the details of the model we use to fit the SEDs, and then we present our strategy for deducing disk structure from the comparison of models and data.

3.1. The Model

We follow what has become a common approach to modeling infrared and submillimeter disk emission (e.g., Adams et al. 1988, hereinafter ALS88; Adams et al. 1990; BSCG). Unless otherwise stated, we use the model of ALS88. We assume an axisymmetric, geometrically thin disk with a power-law surface-density distribution:

$$\Sigma(r) = \Sigma_0 (r/r_0)^{-p}. \tag{1}$$

We use $p = 1.5$ in all models. The disk extends from an inner radius r_0 to an outer radius R_d; we use $r_0 = R_*$ and $R_d = 100$ AU. With these radii fixed, the value of Σ_0 then determines the disk mass M_d.

The disk absorbs and reprocesses stellar photons; reprocessing alone gives a radial temperature distribution that approaches $T \propto r^{-0.75}$ when $r \gg R_*$. The disk may in addition have intrinsic luminosity $L_{\rm disk}$, which is distributed through the disk such that the temperature distribution it produces is characterized by a power-law (cf. ALS88 Eq. 10):

$$T_D(r) \propto r^{-q_d}, \tag{2}$$

with $0.50 \leq q_d \leq 0.75$. The overall temperature distribution of the disk used in the model calculations is set by the combination of reprocessing and intrinsic luminosity. In order to show the combined effects of reprocessing and intrinsic luminosity, we fit the temperature distribution with a power law

$$T(r) = T_1(r/(1\ \mathrm{AU}))^{-q} \tag{3}$$

and report T_1 and q for each model. The emission from the disk is given by

$$F_\nu = \frac{\cos i}{D^2}\int_{r_0}^{R_d} B_\nu[T(r)](1 - e^{-\tau_\nu(r)})2\pi r\, dr, \tag{4}$$

where D is the distance from the observer to the system, i is the angle between the line of sight and the normal to the disk plane, and τ_ν is the line-of-sight optical depth through the disk, related to the mass opacity κ_ν by

$$\tau_\nu(r) = \frac{\kappa_\nu \Sigma(r)}{\cos i}. \tag{5}$$

In the optical and infrared, we use the opacity function calculated by Pollack et al. (1994) for dust in disks around young stars. This is joined smoothly to a power-law opacity function[4] at far-infrared and millimeter wavelengths,

$$\kappa_\nu = 0.1 \left(\frac{\lambda}{250\ \mu\mathrm{m}}\right)^{-\beta}\ \mathrm{cm}^2\,\mathrm{g}^{-1}. \tag{6}$$

This opacity uses the normalization given by Hildebrand (1983), which includes an assumed gas-to-dust ratio of 100:1 by mass. We use $\beta = 1$, roughly the mean value found for T Tauri disks by Beckwith & Sargent (1991).

---

[4]For consistency with previous work, we have used a power-law millimeter-wave opacity function rather than the opacity calculated by Pollack et al. (1994). This allows the disk masses determined from our modeling to be compared directly with those calculated for disks around young stars by other authors (e.g. BSCG). The millimeter-wave opacity function we use is qualitatively similar to that of Pollack et al. (1994); their spherical-grain, 100 K model (the coolest temperature for which they calculate opacities) has $\kappa_\nu = 0.1\ \mathrm{cm}^2\,\mathrm{g}^{-1}$ at $\lambda = 250\ \mu$m and a slope of $\beta = 1.2$ for $\lambda > 1$ mm, but it has a somewhat steeper slope at $\lambda < 1$ mm and is thus a factor of nine lower than our power-law model at $\lambda = 1.3$ mm. Given that most of the mm-wave emission in our models comes from regions in the disks with temperatures below 100 K, the difference between our opacity and the 100 K model of Pollack et al. is consistent with the finding of Agladze et al. (1994, 1996) that κ_ν increases with decreasing temperature.

To simulate disk clearing by a binary companion, we follow Mathieu et al. (1991) in introducing a gap in this disk model. For a model binary-disk system, we set the disk surface density (and thus the emission) equal to zero between radii $r_{\rm in}$ and $r_{\rm out}$, designating the inner and outer edges of the gap:

$$\Sigma(r) = \begin{cases} 0, & \text{if } r_{\rm in} < r < r_{\rm out}; \\ \Sigma_0 (r/r_0)^{-p}, & \text{otherwise.} \end{cases} \tag{7}$$

These radii are determined by the parameters of a given binary system, especially the binary semi-major axis a and eccentricity e. We use the models of Artymowicz & Lubow (1994; their Figs. 3 and 4) to determine $r_{\rm in}$ and $r_{\rm out}$. For the binaries 162814−2427, 162819−2423S, and AK Sco, all of which have eccentricities of $e \sim 0.4$ (see Table 1), we use $r_{\rm in} = 0.2a$ and $r_{\rm out} = 3.0a$. For binaries with circular orbits, such as V4046 Sgr, we use $r_{\rm in} = 0.4a$ and $r_{\rm out} = 1.8a$. The values adopted are given in Table 5. For simplicity in discussing the cleared regions in disks, we define two terms. If a circumstellar disk is present, we will refer to the cleared region between circumstellar and circumbinary disks as a *gap*; if no circumstellar disk is present and the cleared region extends from the stars out to the circumbinary disk, we will refer to it as a *hole*.

The emission from the stars is modeled using a model stellar atmosphere with solar metallicity and main-sequence surface gravity.[5] The model atmosphere is convolved with standard $UBVR_cI_cJHK$ filter profiles to allow direct comparison with the photometric data. Both star and disk emission are reddened using a specified visual extinction A_V (adopted from values given in the literature) and the extinction law of Cardelli et al. (1989) with $R_V = 3.1$.

This model assumes a single star with a circumstellar disk, which is an azimuthally symmetric system; adding another star destroys this symmetry. However, we argue that the emission from a binary-disk system is adequately approximated by a centrally-illuminated, axisymmetric disk with an annular gap, as in this model. To see this, consider the two extreme cases of binary mass ratios. If the masses of the two stars are very different, the orbit of the primary star is very small due to its greater mass, and the luminosity of the primary will be much greater than that of the secondary. Thus, the disk is heated primarily by one star which remains near the center of the disk at all times; such a system is well-approximated by an axisymmetric, centrally-heated disk, perhaps with a gap.

In a binary whose mass ratio is close to one, the two stars contribute more equally to

[5]The atmospheres used were calculated by R. L. Kurucz and were obtained on the World Wide Web at http://www.stsci.edu/ftp/instrument_news/Observatory/k93models.html. They are similar to the models of Buser & Kurucz (1992).

heating the disk due to their similar luminosities and orbits. Near either star or far from the binary center of mass the disk heating is comparable to that in the single star model. However, at distances within a factor few times the binary semi-major axis, the radiation field is more complicated. In the models with cleared gaps or holes (Sec. 3.2) there is no disk material at these radii and so the point is moot. The continuous disk model, however, clearly oversimplifies the radial variation of disk temperature at these distances and should be judged with caution. In addition, these arguments may not be valid for other sources of disk luminosity such as accretion.

3.2. Modeling strategy

Certain model parameters are fixed by additional observations. We take values of A_V from the literature. Spectral types from the literature are used to determine the stellar temperature T_* based on the values given by Lang (1992) for main-sequence stars. Using this value of T_*, the stellar luminosity L_* is determined from a model atmosphere (reddened by A_V) fit to the B, V, and R data. The inclination i of the disk is assumed to be the same as the inclination of the binary orbit. The inclination for each double-lined binary is set by comparing the value of $M_* \sin^3 i$ from the spectroscopic orbit with the theoretical stellar mass M_* derived from the observed spectral type and luminosity; for single-lined systems we use the observed mass function to constrain the inclination. The inclination is very uncertain, but it is held fixed for each binary and therefore does not affect the comparison of different models of the same system.

Having fixed these parameters, we then compare the observed infrared SED of each of our target binary systems (see Sec. 2) with several different models, discussed in the following paragraphs. Our goal is to determine whether the disks have regions that are cleared of material, and each model is designed to test a specific hypothesis about a possible arrangement of disk material.

First, we compare the data to a model of an optically thick reprocessing disk with no holes or gaps. This idealized model is arguably the simplest physically plausible disk model, and thus it serves as a point of reference for our later comparison of the data with more sophisticated models. We calculate the emission from a disk that is optically thick at visible and infrared wavelengths and is continuous from the stellar surfaces to the outer radius. L_* is fixed by the BVR data and the model has no other free parameters. We assume that the disk has no source of energy other than the reprocessing of stellar photons ($q \to 0.75$ at radii $r \gg R_*$). Such a disk has the minimum luminosity possible for an optically thick disk; the disk cannot be cooler than this (accretion or increased spatial thickness will only increase its temperature) and therefore cannot be less luminous unless it becomes optically thin. Thus, if the observed emission from a system at a given wavelength falls below this model, the disk *must be optically thin* in the regions that dominate the disk emission at that wavelength. In particular, if the disk emission falls below this model at near- or mid-infrared wavelengths but at or above it at longer wavelengths, the disk must have a gap or hole in it in order to explain the deficit of short-wavelength emission.

While emission that falls below this "continuous reprocessing disk model" clearly reveals the presence of a gap or hole, failure to meet this criterion does not mean that a gap or hole is not present. In particular, if the disk temperature profile inferred from the SED is flatter than $q = 0.75$ (as is the case in most T Tauri disks; Strom et al. 1989, BSCG), the disk emission may not fall below the reprocessing disk model at any wavelength even if a gap or hole is present. Nonetheless the SED will show a dip (see e.g. the GW Ori SED in Mathieu et al. 1991, 1995).

We next allow $L_{\rm disk}$ and q_d to be free parameters in fitting the data (thereby determining T_1 and q; see Eqs. 2 and 3). We also allow the disk mass M_d to vary to fit the submillimeter and/or millimeter data. We calculate three model SEDs: one from a continuous disk, one from a disk with a gap cut in it from $r_{\rm in}$ to $r_{\rm out}$ and one from a disk with a central hole of radius $r_{\rm out}$. For brevity, we refer to these subsequently as the continuous active disk model, the dynamic gap model, and the dynamic hole model. All three models have the same number of free parameters (three), since the locations of the cleared regions are fixed by theory. Comparing these models therefore allows an assessment of whether the structure of the SED is better fit by a disk with or without a cleared region, and whether the observed SED is well matched by the predicted emission from a model that incorporates the theoretically-expected disk clearing.

Finally, we calculate a spectral energy distribution using a model in which the gap size is allowed to vary. This allows us to determine if the values of $r_{\rm in}$ and $r_{\rm out}$ that best fit the data specify a gap or hole location that is on the same size scale as the orbit of the binary. We do not suggest that these values of $r_{\rm in}$ and $r_{\rm out}$ are the exact gap radii present in the disk. Small differences in gap locations are within the uncertainties set by the observational data and limitations imposed by the simplicity of the model; however, large differences between predicted and fit values of $r_{\rm in}$ and $r_{\rm out}$ may suggest that the observed structure in the SED is not due to an empty gap cleared by the binary.

In each of these fits, we employ a variant of the Levenberg-Marquardt algorithm (e.g. Press et al. 1992) to find the set of model parameters that minimizes the root mean squared deviation of the model from the data points. In the fitting we have weighted all points equally rather than weighting by the formal uncertainties, since the true uncertainty on the fluxes is probably dominated by the (poorly known) variability. We do not give specific χ^2 values for the models as a measure of goodness-of-fit since in general even the better models do not give χ^2 values that indicate good agreement with the data. This is most likely a result of the simplicity of our model compared to the more complex conditions in real binary-disk systems. Nonetheless, this method gives us an objective measure of the relative quality of various fits.

4. Models for Specific Binary Systems

We now apply the models discussed above to specific binary systems. For each system we give a brief background, discuss the adopted system parameters (see Table 5) and sources of the photometry used, and present the model-fitting results.

4.1. 162814−2427

The double-lined spectroscopic binary 162814−2427 lies in the ρ Oph star-forming region at a distance of 125 pc (de Geus et al. 1989). Lee (1992) placed 162814−2427 on an HR diagram and found component masses of $M_1 = 1.2\ M_\odot$ and $M_2 = 1.1\ M_\odot$ using the models of D'Antona & Mazzitelli (1994).[6] Using these masses and $M \sin^3 i = 1.96\ M_\odot$ from Mathieu et al. (1989) we find an inclination of $i = 71°$. The binary semi-major axis is then $a = 0.28$ AU, and the predicted extent of a dynamically cleared gap is from $r_{\rm in} = 0.057$ AU to $r_{\rm out} = 0.85$ AU.

The 162814−2427 system varies by up to 0.4 magnitudes at V (Lee 1992) and K (Walter et al. 1994) with no discernible periodicity (Zakirov et al. 1993). We adopt the brightest set of $UBVR_cI_c$ data (see Sec. 3.2), that given in Lee (1992); the data are reproduced in Table 6. Infrared photometry was taken from our own observations and Walter et al. (1994). *IRAS* data were taken from Clark (1991), and an 800 μm upper limit from Jensen et al. (1996a). A spectrum of the system from 8–13 μm shows no silicate feature; a conservative upper limit on the strength of any weak silicate emission would be < 0.25 the strength of the emission feature in AK Sco (Jensen & Mathieu, unpublished data).

The 162814−2427 system is a hierarchical triple. Lee (1992) discovered the third star

[6]The somewhat earlier spectral type found by Lee (1992; Table 5) resolves the conflict between dynamical and theoretical mass limits found by Mathieu et al. (1989), who used a spectral type of K7 for 162814−2427.

spectroscopically, and Ghez et al. (1993) independently discovered the third star using infrared speckle observations. The tertiary component has an approximate spectral type of K5 and is roughly a factor of five fainter than the combined primary and secondary at 0.6 μm (Lee 1992) and 2.2 μm (Ghez et al. 1993). The angular separation of $0''\!.15$ (Ghez et al. 1993) corresponds to a projected physical separation of $\sim$ 20 AU, much greater than the average primary-secondary separation of 0.3 AU. All of the photometry we use includes all three stars; complications in modeling introduced by the presence of the tertiary are addressed below.

Figure 1 shows the results of fitting various models to the 162814−2427 SED. Figure 1(a) shows the continuous reprocessing disk model. None of the data fall below the model, and therefore there is no requirement that the inner regions of the disk be optically thin. However, the complex structure of the SED is clearly not well-fit by this model.

Figures 1(b)–1(d) compare models with differing spatial distributions of disk material. Panel (b) shows the best fit with a continuous disk ($q = 0.51$, $T_1 = 190$ K, $L_{\rm disk} = 0.45\ L_\odot$); panel (c) shows the best fit with a disk that has a gap from $r_{\rm in} = 0.057$ AU to $r_{\rm out} = 0.85$ AU ($q = 0.54$, $T_1 = 230$ K, $L_{\rm disk} = 0.69\ L_\odot$); and panel (d) shows the best fit with a hole extending to $r_{\rm out}$ ($q = 0.75$, $T_1 = 270$ K, $L_{\rm disk} = 0.25\ L_\odot$). The dynamic gap model clearly fits the data better than the continuous active disk model, demonstrating that the SED structure is consistent with the presence of a gap of the size predicted by disk models.[7] We emphasize that the gap size is *not* a free parameter in this model fit; if the gap size is allowed to vary, the best fit is found for $r_{\rm in} = 0.047$ and $r_{\rm out} = 0.40$, similar to the dynamically predicted gap and encompassing the binary orbit. Finally, the dynamic hole model in Fig. 1(d) does not fit the data well because it does not reproduce the observed near-infrared excess.

The presence of a tertiary star adds some ambiguity to these conclusions. For example, the small near-infrared excess could derive from the tertiary star, in which case the binary might have no circumstellar disk(s) at all. We cannot rule out this possibility. More broadly, both the near-infrared excess and the much larger 10–60 μm excess could arise from a disk around the tertiary, with no disk material associated with the binary. We stress, however, that the tertiary is visible in the optical, so it is not an "infrared companion". Furthermore at both optical and infrared wavelengths the companion is substantially fainter than the binary. Finally, associating all of the infrared excess emission with the tertiary would not alter our conclusion that the SED structure is best fit by a disk with most of its inner

[7]We note that none of the models can fit both the 20 μm point and the *IRAS* 25 μm point. The discrepancy between these may reflect the variability of the source, unaccounted for in our model.

region cleared of material. The presence of a centrally-cleared disk around the tertiary is unmotivated *a priori* but not out of the question (see Sec. 5.4).

We conclude that the most likely model for the 162814−2427 system is a disk associated with the binary in which is a central cleared region that encompasses the binary orbit. Even so, the presence of the tertiary cannot be ignored since at a projected separation of ~ 20 AU it too must interact with the circumbinary disk. This may explain the lack of submillimeter emission from this system (Jensen et al. 1996a).

4.2. V4046 Sgr

V4046 Sgr was discovered to be a double-lined spectroscopic binary by Byrne (1986) and de la Reza et al. (1986). It is not associated with any known region of star formation, but it does show characteristics typical of classical T Tauri stars: strong, variable Hα emission (equivalent width 30–120 Å), strong Li absorption, and ultraviolet, infrared, and millimeter excesses (Byrne 1986, de la Reza et al. 1986, Jensen et al. 1996a). It is thus similar to other isolated T Tauri stars such as TW Hya (Rucinski & Krautter 1983, Gregorio-Hetem et al. 1992). For this discussion we consider it as a PMS star, but we note that its PMS status is less certain than for the other binaries in our sample and its distance is unknown.

The system varies at V with an amplitude of 0.06 mag and a period that is roughly equal to the binary period (de la Reza et al. 1986, Byrne 1986). There is also aperiodic variability at U and B, with occasional flares at U (Busko & Torres 1976). We adopt the brightest UBV magnitudes from Busko & Torres (1978) (not including the brightest flare of 0.7 mag at U, Busko & Torres 1976) and the R_c and I_c magnitudes from Hutchinson et al. (1990). Infrared photometry is taken from Hutchinson et al. (1990) and our own observations, *IRAS* fluxes from Weaver & Jones (1992), and submillimeter photometry from Jensen et al. (1996a). Narrow-band photometry of the system from 8.75–11.5 μm (Hutchinson et al. 1990) shows a marginal very weak silicate emission feature. Given the large uncertainty of this detection we will not consider silicate emission in our modeling.

The brightest measured V magnitude of the system in the literature is $V = 10.32$. Combined with the luminosity ratio of 1.7 (Lee 1994), this yields $V = 10.9$ for the primary. Assuming a spectral type of K5 for the primary (de la Reza et al. 1986) and taking $M_V = 7.4$ for the absolute V magnitude of a main-sequence K5 star (Lang 1992) we obtain a distance of 50 pc to V4046 Sgr. Since the true luminosity of V4046 Sgr is higher if it is a pre–main-sequence system, this distance estimate is a lower limit to the true distance. We adopt this distance limit for discussion purposes. No value of A_V is given in the literature. The mean $B - V$ color is near normal for a K5 star, so we adopt $A_V = 0$. The adopted inclination (Table 5) yields $a = 0.04$ AU, and $r_{\rm in} = 0.016$ AU and $r_{\rm out} = 0.072$ AU for the expected gap location given the system's circular orbit.

Fits to the SED of V4046 Sgr are shown in Fig. 2. Panel (a) shows the continuous reprocessing disk model. The fluxes at all wavelengths shortward of 10 μm are photospheric. The 1–5 μm fluxes fall well below the reprocessing disk model, indicating that the inner regions of the V4046 Sgr disk are optically thin. The observed variability may indicate a small near-infrared excess if the brightest magnitudes at JHK are adopted, but all measured 1–5 μm fluxes are well below the model in all observations so an optically thin region in the inner disk is required.

Models with differing disk structure are shown in panels (b) ($q = 0.51$, $T_1 = 90$ K, $L_{\rm disk} = 0.03\ L_\odot$), (c) ($q = 0.51$, $T_1 = 100$ K, $L_{\rm disk} = 0.03\ L_\odot$), and (d) ($q = 0.51$, $T_1 = 100$ K, $L_{\rm disk} = 0.02\ L_\odot$). Neither model (b) (continuous active disk) nor (c) (dynamic gap) fits the data well, since both have too much near-infrared emission. However, model (d), with a cleared inner hole out to the dynamically predicted $r_{\rm out}$, fits the data well.[8] If $r_{\rm in}$ and $r_{\rm out}$ are allowed to be free parameters in fitting the SED, the best fits are for values of $r_{\rm in} = R_*$ and $r_{\rm out} = 0.18$ AU. This hole is larger than the dynamically predicted value, but not greatly so, and encompasses the binary orbit.

We conclude that V4046 Sgr has a circumbinary disk with a central hole of a size consistent with dynamical clearing by the binary. The complete lack of near-infrared excess makes the conclusion of central clearing quite model-independent.

4.3. 162819−2423S

The 162819−2423S system is a single-lined spectroscopic binary (Mathieu et al. 1989) in the ρ Oph cloud. It is part of a hierarchical quadruple system, lying $4\farcs8$ from 162819−2423N (ROXs 43B), a $0\farcs016$-separation binary (Simon et al. 1995). Because 162819−2423S is a single-lined binary, its orbital inclination is more difficult to estimate than the double-lined systems discussed above. Using a mass of 1.3 $M_\odot$ for the primary and $f(m) = 0.017\ M_\odot$ (Mathieu et al. 1989), inclinations $i < 22^\circ$ give secondary masses

[8]As in the case of 162814−2427, there are discrepancies between the ground-based 10 and 20 μm points and the *IRAS* 12 and 25 μm points, possibly reflecting source variability or extended emission in the larger *IRAS* beam (Sec. 5.4). None of the models (including the dynamic hole model) matches the mid- and far-infrared data well.

greater than the primary mass, which is unlikely. We adopt $i = 60°$, the mean inclination for systems with randomly-distributed orbits, but note that this is highly uncertain.

The only optical photometric data for 162819−2423S in the literature are those of Mathieu et al. (1989), which do not resolve the N-S pair. New, resolved $UBVR_cI_c$ photometry of 162819−2423S is given in Table 6. We used this photometry to derive an extinction of $A_V = 2.4$, consistent with the estimate of $A_V = 2.3$ by Bouvier & Appenzeller (1992); we did not adopt the values of A_V from Mathieu et al. (1989) or Walter et al. (1994) since they are based on the combined light of 162819−2423S and 162819−2423N and do not fit the new data well. Infrared photometry was taken from our observations and from Walter et al. (1994); both sources contain photometry out to $\lambda = 20$ μm that resolves 162819−2423S from 162819−2423N. Because of the availability of resolved data and the fact that *IRAS* data do not resolve the N-S pair, we do not include the *IRAS* 12- and 25-μm points. However, in the absence of other data at longer wavelengths we do adopt the unresolved *IRAS* 60 μm flux (Clark 1991). We assume that most of the observed 60 μm flux comes from 162819−2423S rather than 162819−2423N, since 162819−2423S is brighter at all infrared wavelengths where the pair is resolved with the N-S flux ratio increasing with wavelength to 4:1 at 10 μm, the longest wavelength at which a flux for 162819−2423N is available. Also, the unresolved *IRAS* 25 μm flux is less than 20% above the resolved 20 μm flux from 162819−2423S, indicating that there is little contribution from 162819−2423N at this wavelength. An 800-μm upper limit is taken from Jensen et al. (1996a).

162819−2423S has a prominent 9.8–μm silicate emission feature (Fig. 5) like those seen in many other T Tauri stars (Cohen & Witteborn 1985). The presence of this emission feature suggests a somewhat more complicated temperature and/or surface-density distribution in the disk(s) than we have assumed in the previous systems. Our "standard" models, whose 10 μm emission is produced by optically thick regions in the disks, do not produce any emission features and thus cannot match the observations. For comparison with our results in modeling the other systems, we first test the ability of the standard models to match the SED using the broad-band N flux at 10 μm, and then explore an extension of the model to match the silicate emission (using the narrow-band 7.8–12.5 μm data in place of the N flux).

Figure 3 shows our standard suite of models for 162819−2423S. The data fall below the reprocessing disk model [Fig. 3(a)] from 1–5 μm, suggesting an optically thin inner disk. Given the large uncertainty in the inclination of 162819−2423S, this model could be inaccurate; an inclination of $i = 69°$ yields a reprocessing disk model that matches the 1–5 μm data. Regardless of inclination, however, the SED resembles that of 162814−2427 and does not have a power-law slope.

Figures 3(b)–3(d) show the other models. Among these models, the continuous active disk [Panel (b); $q = 0.51$, $T_1 = 220$ K, $L_{\rm disk} = 0.74\ L_\odot$] cannot match the observed inflection in the SED at 5 μm. Both the dynamic gap model [Panel (c); $r_{\rm in} = 0.023$ AU, $r_{\rm out} = 0.35$ AU, $q = 0.57$, $T_1 = 280$ K, $L_{\rm disk} = 1.35\ L_\odot$] and the dynamic hole model [Panel (d); $q = 0.75$, $T_1 = 280$ K, $L_{\rm disk} = 0.72\ L_\odot$] match the data reasonably well, though the former produces too much near-infrared excess and the latter not enough. A fit with the gap size as a free parameter yields $r_{\rm in} = 0.049$ AU, $r_{\rm out} = 0.24$ AU, somewhat smaller than the dynamically predicted gap, but encompassing the binary orbit.

Mathieu et al. (1991, 1995) suggested that the strong silicate emission feature in GW Ori might arise from optically thin dust in a gap cleared by the binary companion. Motivated by this suggestion and the presence of strong silicate emission in 162819−2423S, we now explore whether a model with a gap that is not entirely cleared can provide an adequate fit to the SED. For simplicity, we assume that the dust in the gap or hole is isothermal with temperature $T_{\rm gap} = 1000$ K and has uniform surface density, parameterized by τ_{10}, the optical depth at $\lambda = 10\ \mu$m (the peak of the silicate feature). The total mass of dust is therefore set by τ_{10}, $r_{\rm in}$, and $r_{\rm out}$.

Figure 5(a) shows the dynamic hole model with optically thin dust added to the cleared region. The model provides a reasonable fit to the observations, producing a silicate emission feature while still matching the SED at other wavelengths. The absolute strength of the silicate emission feature is not well-reproduced; we discuss this further in Sec. 4.4. Very little mass is needed to produce the emission feature; the model shown has $\tau_{10} = 0.2$, corresponding to a mass of $\sim 10^{-9}\ M_\odot$ of optically thin material in the hole.

To summarize, the SED of the 162819−2423S system is best fit by models that have the dynamically expected gap or hole size. The dynamic gap and hole models provide reasonable fits to the SED even without the addition of optically thin dust; adding dust to the hole reproduces the silicate emission feature while still fitting the continuum emission at other wavelengths. Thus we conclude that 162819−2423S likely has a gap or hole in its disk.

4.4. AK Sco

AK Sco was discovered to be a double-lined spectroscopic binary by Andersen et al. (1989). It is projected on the outskirts of the Upper Sco star-forming region, and Andersen et al. (1989) argue that it is a member of Upper Sco based on its proper motion and radial velocity. The distance to Upper Sco is 160 pc (de Geus et al. 1989), and we adopt this as the distance to AK Sco. The adopted inclination (Table 5) yields predicted gap radii of $r_{\rm in} = 0.032$ AU and $r_{\rm out} = 0.48$ AU.

We compiled photometric data for AK Sco from Kilkenny et al. (1985), Andersen et al. (1989), Herbst et al. (1994), Hutchinson et al. (1994), our own photometry, Weaver & Jones (1992), and Jensen et al. (1996a). AK Sco is highly variable at optical (Andersen et al. 1989) and infrared (Hutchinson et al. 1994) wavelengths. The variations are uncorrelated with binary orbital phase and are apparently aperiodic. There is a clear variation of color with optical brightness (the system is redder when it is fainter), suggesting variable obscuration by circumstellar or circumbinary dust (Andersen et al. 1989). AK Sco has also been observed to brighten at 10 μm when the optical flux decreases (Hutchinson et al. 1994).

As with 162819−2423S, AK Sco shows a strong 9.8-μm silicate emission feature. We again first model the broad-band SED using the N flux and subsequently model the silicate feature.

Figure 4 shows the four standard models and their best fit to the AK Sco SED. The reprocessing disk model [Fig. 4(a)] falls above the 1–2 μm fluxes, though not greatly so, indicating a possible optically thin region near the stars. However, given the relatively small distance between data and model and the known variability of AK Sco, we cannot securely conclude from this model that AK Sco must have any optically thin regions in its disk.

Indeed, unlike the previous three systems, neither the dynamic gap [Fig. 4(c); $q = 0.59$, $T_1 = 360$ K, $L_{\rm disk} = 4.41\ L_\odot$] nor dynamic hole [Fig. 4(d); $q = 0.75$, $T_1 = 420$ K, $L_{\rm disk} = 2.57\ L_\odot$] model provides a good fit to the broad-band data, while the continuous active disk model [Fig. 4(b); $q = 0.51$, $T_1 = 290$ K, $L_{\rm disk} = 2.31\ L_\odot$] fits fairly well. A model in which the gap size is a free parameter yields the unphysical values $r_{\rm in} = 0.015$ AU and $r_{\rm out} = 0.046$ AU, to be compared to the binary semi-major axis of 0.16 AU. Therefore, following our "standard model" approach to SED modeling, there is no evidence for disk clearing in the AK Sco system.

However, interpretation of these results is complicated by the presence of strong silicate emission. As above, we now calculate models with an added component of optically thin dust in the cleared regions of the dynamical models. We fix $T_{\rm gap}$ at 1000 K, roughly the expected equilibrium temperature for optically thin dust at a few tenths of an AU from an F5 star. The resulting fit is shown in Fig. 5(b), where $\tau_{10} = 0.4$ corresponding to $\sim 10^{-9}$ $M_\odot$ of material in the hole. The model provides a very good fit to the continuum emission, and a silicate emission feature at 10 μm. Thus, with a small modification a model with the dynamically expected clearing can qualitatively match the observed data.

As with 162819−2423S, the silicate emission of the models is not as large as observed. We have explored whether this could be the result of the particular dust opacity model we used, and we conclude that it is not. The choice of opacity function does have an effect on the calculated SEDs, since the addition of opacity at wavelengths near 10 μm from non-silicate grain species can reduce the strength of the silicate emission feature (Pollack et al. 1994). For example, the opacity used by ALS88 has both silicate and graphite opacity at 10 μm, and thus has a somewhat smaller silicate feature than the opacity used here; this opacity was used by Mathieu et al. (1991, 1995), who also had difficulty matching the observed silicate emission strength in the GW Ori SED. However, we use the opacity calculated by Pollack et al. (1994) for 1000 K dust in circumstellar disks. In this model, almost all the 10 μm opacity is provided by silicates, producing a large feature in the opacity profile. Comparison of the Pollack opacity with opacity from pure silicates (Jäger et al. 1994) shows that the two have similar emission features; models calculated with the pure silicate opacity do not fit the observed features better. Thus, our inability to match the strength of the silicate emission is unlikely to be simply an artifact of the particular dust opacity model we used.

The strength of the observed emission features suggests that the silicate emission is produced by relatively hot dust; Pollack et al. (1994) find that at temperatures below about 500 K the strength of the emission feature is greatly reduced due to added opacity from other grain species [see their Fig. 3(b)]. This corresponds well with our assumed dust temperature of 1000 K; however, our poor match to the silicate features may reflect the overly simple dust distribution (isothermal and isodensity) assumed in our models. Indeed, a stronger silicate emission feature could be achieved if the optically thin material were not confined to the disk plane. For AK Sco, the observed trend of redder colors accompanying fainter optical magnitudes suggests variable circumstellar extinction (Andersen et al. 1989, Hutchinson et al. 1994). This has been attributed to "clumpy accretion" of material outside the disk plane (Herbst et al. 1994).

Our conclusions about the disk structure in AK Sco are twofold. First, the system apparently does not have an entirely evacuated gap or hole in the region of the binary orbit. Second, the lack of such an evacuated region does not necessarily imply that no disk clearing has occurred in the system. The addition of a relatively small amount of optically thin material ($\sim 10^{-9}\ M_{\odot}$) in a central hole, motivated by the presence of strong silicate emission, provides a reasonably good fit to the SED. Thus AK Sco *could* have a central hole in its disk of the size predicted by disk dynamics. This would require that AK Sco is not as efficient at entirely clearing this inner region of material as are 162814−2427 or V4046 Sgr.

4.5. Calculation of Disk Masses

We calculated disk masses for these systems as part of the disk modeling discussed above. The disk mass was allowed to be a free parameter in the model fits. The disk is optically thin only at submillimeter and millimeter wavelengths, so only those data influenced the derived disk mass, while the temperature was set by the infrared data. The disk masses derived from the model fits are given in Table 7. In each case we have used the mass from the model that best fits the data as discussed above; however, the masses from the various models did not differ by more than a factor of two, well within the uncertainty[9] in the millimeter opacity.

5. Discussion

5.1. Cleared Regions in Disks

The theory of binary-disk interactions predicts that binaries clear holes or gaps in their disks. This in turn implies that short-period binaries will show deficits of near-infrared emission. We have found that the SEDs of three short-period PMS binaries show such deficits. Furthermore, synthetic SEDs calculated from disk models with gaps or holes at the dynamically predicted locations agree with these observed SEDs. A similar conclusion was drawn for the PMS binary GW Ori (Mathieu et al. 1991).

At the same time, the SED of the binary AK Sco shows no evidence for a deficit of near-infrared emission, despite having an orbital period and eccentricity similar to those binaries showing deficits. Even so, both the silicate emission and the SED can be fit by a disk model having a hole within which resides optically thin dust. Two other short-period binaries in our parent sample show SEDs similar to AK Sco. The binary DQ Tau has recently been studied intensively (Mathieu et al. 1997, Basri et al. 1997). Its power-law infrared SED, even in the near infrared, gives no indication that the inner region of the disk is cleared by the binary. As with AK Sco, such clearing is not precluded; very little material is required to produce the observed near-infrared emission and the data are consistent with residual material in a dynamically cleared hole. At present it is not known whether DQ Tau has silicate emission. The binary UZ Tau E also shows a power-law-like SED and silicate

[9] Various laboratory measurements and dust models yield values for $\kappa_\nu(1.3\ \mathrm{mm})$ that vary by an order of magnitude depending on the dust model, composition, and temperature. For recent work on the millimeter opacity of circumstellar dust, see Pollack et al. (1994), Krügel & Siebenmorgen (1994), and Henning & Stognienko (1996) for theoretical calculations and Agladze et al. (1994, 1996) for laboratory measurements.

emission (Ghez et al. 1994). Aside from the silicate emission the SED of UZ Tau E is well fit by a continuous active disk (Jensen et al. 1996b). Again, the silicate emission and SED can also be fit with a partially evacuated hole having the dynamically appropriate outer radius.

In summary, well-sampled SEDs are available for seven of the nine known binaries with separations less than 1 AU. Of these, four binaries show structure in their SEDs consistent with cleared regions of sizes predicted by dynamical theory. Three binaries do not show such structure and hence their SEDs do not *require* the presence of cleared regions. However gaps or central holes are still permitted if they are not entirely empty; indeed silicate emission features in two of the cases may be indicative of optically thin dust in cleared regions. In any case, these three binaries demonstrate that binary-disk interactions and the origin of near-infrared emission are more complex than previously thought.

5.2. Circumstellar Disks

Most of the binaries in our parent sample have near-infrared excesses which reveal the presence of hot material near the stars. This is a significant result in and of itself, for close binary companions are thought to severely limit the radii of any circumstellar disks. For example the predicted inner gap radii of the four binaries studied here are all less than 0.06 AU, and in several cases are only a few stellar radii. Indeed these inner gap radii may lie within the magnetospheric radii for these active stars (e.g., Königl 1991, Shu et al. 1994). Thus while formally circumstellar disks may be modeled for these systems in the context of cleared gaps, the actual physical situation is almost certainly more complicated.

Furthermore, dynamical clearing has been thought to cut off circumstellar regions from replenishment by material from circumbinary disks (e.g., Artymowicz et al. 1991). If so, then typical accretion rates (i.e. comparable to those inferred for single stars) or Poynting-Robertson drag on optically thin material would exhaust the circumstellar material in these close binaries on timescales shorter than their 10^5–10^6 year ages (Simon et al. 1993, Lubow & Artymowicz 1996).

Nonetheless, based on their near-infrared excesses circumstellar material is present in these close binaries. Given the high emissivity of dust in the near-infrared, very little mass is needed to reproduce the near-infrared excesses in these binary systems. In the models for 162819−2423S and AK Sco (Fig. 5), the total mass of material in each of the central holes is only $\sim 10^{-9}\ M_{\odot}$. The spatial distribution of the near-infrared-emitting material is largely unconstrained and need not be disk-like. It is likely that continuous replenishment is required.

Recently, a possible mechanism for transferring material from circumbinary disks into the region of the binary orbit has been suggested by Artymowicz & Lubow (1996). In their model, circumbinary disks with sufficiently large vertical scale heights and viscosities may form pulsed "accretion streams" between circumstellar and circumbinary disks. A gap forms between circumstellar and circumbinary disks, but it is not entirely empty of material; some material continues to flow from the circumbinary disk through the gap. This mechanism can support relatively large accretion rates, comparable to those inferred for continuous disks around single stars.

DQ Tau has proved to be an interesting testbed for this theory (Mathieu et al. 1997, Basri et al. 1997). Periodic variability in broad-band light, spectral veiling, and Hα emission all suggest that the mass accretion rate increases at periastron passage, coincident with the predicted infall of the pulsed accretion streams onto the stars. At the same time there is lower-level veiling present throughout the orbit, indicating a continuous source of circumstellar material as well.

If such "leakage" from circumbinary disks is a common phenomenon, then it may provide a general explanation for the near-infrared excesses seen among these close binaries. Most if not all of these binaries have circumbinary disks (Sec. 5.3), so there is a mass reservoir available to supply the material. The critical issue is whether the circumbinary disks in DQ Tau or any binary system have the vertical scale heights and viscosities required by the Artymowicz & Lubow model for mass flow across gaps.

Given how little mass is required to produce a near-infrared excess, it is remarkable how completely cleared the region around V4046 Sgr appears to be. All of the fluxes from the optical through 5 μm are consistent with purely photospheric emission. This utter lack of near-infrared excess is doubly interesting given that V4046 Sgr shows a large Hα equivalent width (30–120 Å; Byrne 1986). Strong Hα emission is often interpreted as an indicator of accretion in T Tauri stars, but V4046 Sgr apparently has no material near the stars to accrete. The presence of strong Hα emission with no near-infrared excess is puzzling.[10]

---

[10]This problem is not unique to V4046 Sgr; all five of the PMS single stars identified in Sec. 5.4 as having no near-infrared excesses also have strong Hα emission (Strom et al. 1989).

5.3. Circumbinary Disks and Orbital Evolution

Among the binaries in Table 1, there are six systems (AK Sco, V4046 Sgr, UZ Tau E, V773 Tau, DQ Tau, and GW Ori) with detected submillimeter flux. The submillimeter continuum emission detected in these close binary systems must arise from material outside the binary orbit. For all but V773 Tau, a simple calculation shows that if the binary orbit were filled with optically-thick material emitting at the stellar temperature, the resulting 800 μm flux would still be less than the observed flux by at least an order of magnitude. Thus, the submillimeter-emitting region in these systems must be substantially larger than a few AU in radius and therefore must lie primarily outside the binary orbits. This indirect argument is borne out by $\lambda = 1.3$ mm images of UZ Tau E which show a 150-AU-radius circumbinary disk (Jensen et al. 1996b). In the case of 162819−2423S, the presence of a 60 μm excess suggests the presence of a circumbinary disk through similar reasoning. In the case of V773 Tau and 162814−2427, we cannot conclude that a circumbinary disk must be present because of the presence of a tertiary in the system; while these systems may have circumbinary disks, far-infrared or millimeter emission could arise from a disk around the tertiary alone. W134 has not been detected longward of $\lambda = 12$ μm. Thus, at least six and possibly eight of the nine binaries in Table 1 have circumbinary disks.

The detection of massive circumbinary disks affords the opportunity to test predictions from dynamical theory about the effect of a disk on the orbital elements of a binary. Both theoretical calculations and smoothed-particle hydrodynamics simulations find that a circumbinary disk will increase the eccentricity of a binary orbit if there is sufficient circumbinary disk mass (Artymowicz et al. 1991, Lubow & Artymowicz 1992). Prior to recent surveys of millimeter emission from young binaries (Jensen et al. 1996a, Dutrey et al. 1996) and the detection of several new spectroscopic binaries (Welty 1995, Mathieu et al. 1996, 1997), the only known binary with measured orbital elements and clear evidence for a massive circumbinary disk was GW Ori (Mathieu et al. 1991). The near-circular orbit of GW Ori seems to contradict the theoretical expectation of rapidly increasing eccentricity in the presence of a circumbinary disk (Lubow & Artymowicz 1992, Mathieu et al. 1995).

In fact, GW Ori is the exception rather than the rule among close binaries with circumbinary disks. Among the six binaries in Table 1 with clear evidence for circumbinary disks (Sec. 4.5), only V4046 Sgr has a circular orbit. With an orbital period of 2.4 days, the circularity of the orbit is almost certainly due to tidal circularization. Except for GW Ori, the remainder of the close binaries with circumstellar disks have orbital eccentricities between 0.25 and 0.6. These are typical of all PMS binaries of similar periods. (For a complete discussion, see Mathieu 1994.)

The substantial eccentricities of these binaries could be attributed to the influence of their circumbinary disks. Lubow & Artymowicz (1992; see also Lubow & Artymowicz 1996) find that the rate of eccentricity evolution depends on the relative masses of the binary and the disk material at the resonances near the binary orbit. Specifically, they calculate orbital evolution timescales as a function of the ratio of the binary mass to the mass of the circumbinary disk within a distance of six times the binary semi-major axis from the binary center of mass (their Equation 2). Adopting the disk model used above (with $p = 1.5$ and $r_{\rm out}$ given for each system) and the disk masses derived from the model (Table 7), this ratio is of order 10^{-4}–10^{-5}. This yields a characteristic time $(e/\dot{e})$ for eccentricity excitation on the order of 10^5–10^6 binary orbital periods. Given the short periods of the binaries discussed here this is sufficient to have substantially increased the orbital eccentricities over the 10^5–10^6 year ages of these systems. Thus if these binaries were formed with small orbital eccentricities, the influence of their disks could have produced the eccentricities observed today. In addition, the highest observed eccentricity among these systems is 0.58, consistent with the finding of Lubow & Artymowicz (1992) that the eccentricity-pumping mechanism becomes much less efficient around $e \approx 0.5$. Nonetheless, this consistency is not proof, and it remains equally plausible that the orbital eccentricities derived from the formation process itself.

In addition to increasing the eccentricity, a circumbinary disk may cause a binary's semi-major axis to decrease (e.g., Artymowicz et al. 1991). Using the numbers discussed above and Equation 4.31 of Lubow & Artymowicz (1996) with $\alpha = 0.1$, the characteristic time $(a/\dot{a})$ for semi-major axis evolution of these systems is approximately 8×10^6–8×10^7 orbital periods. This is significantly longer than the timescale for eccentricity evolution and is of the same order of magnitude as the ages of the systems discussed here. These numbers suggest that semi-major axis evolution may not be large for these systems *at present*. However, the timescales calculated above are based on the present conditions in the disks and do not reflect on any past evolution that may have occurred.

5.4. Structure in SEDs as a Diagnostic of Disk Clearing

It is instructive to compare the SEDs of the binaries with those of a sample of single stars, since in the absence of known companions, there is no *a priori* reason to expect cleared regions in the disks around these stars. To compile a sample of single stars with disks for comparison with the binaries, we chose PMS stars from Herbig & Bell (1988) that were detected by *IRAS*. We then chose those stars that were surveyed by at least one of Leinert et al. (1993), Ghez et al. (1993), and Simon et al. (1995) and found to be single. These surveys were sensitive to companions wider than about 10 AU; to eliminate systems with closer companions, we chose only those stars that had also been surveyed spectroscopically (Mathieu, unpublished data) and found not to show radial velocity variability. The result is a set of 13 single stars. We compiled SEDs for these stars from data in Strom et al. (1989), Weaver & Jones (1992), Cohen (1974), and Kenyon & Hartmann (1995). We adopted the spectral type and A_V from Strom et al. (1989) and calculated a continuous reprocessing disk model for each star as discussed above for the binary systems.

Of the 13 single stars, three (CX Tau, DM Tau, and GM Aur) have SEDs that resemble those of V4046 Sgr, with photospheric flux levels from 1–3 μm but excesses at 10–60 μm; two others (DN Tau and BP Tau) have very small K and L excesses, but much larger 10–60 μm excesses. Thus SED structure indicative of a cleared gap or hole is seen in some single stars as well as binaries (see e.g. the SED of GM Aur in BSCG). In addition, only a few of the other single stars have SEDs with the smooth, power-law slopes expected from continuous disks with smoothly decreasing temperatures. Indeed, several of the single stars show SEDs that are similar to those of 162819−2423S, with clear near-infrared excesses but varying degrees of inflection in the 2–10 μm range.

It is apparent, then, that neither the single-star SEDs nor those of binaries conform to the simple paradigm in which single stars show the power-law SEDs of continuous disks having power-law temperature distributions, and close binaries show SED structure indicative of disk clearing. Simply put, it would be difficult to determine from the SED alone whether a given star has a close stellar companion or not. Interestingly, this result is consistent with the finding of Simon & Prato (1995) for wider binaries that inner disk clearing seems to occur at the same rate in single and multiple systems. Before we draw conclusions about the prevalence of disk clearing, however, we must examine several other factors that may contribute to the observed diversity of SED structures. In each case, we discuss the implications for interpretation of the SEDs of both the spectroscopic binaries and the single stars.

One factor that can influence SEDs is variability; in no case was all of the photometry taken simultaneously, and thus variations in flux levels between the different sets of observations could in principle introduce deviations from a power-law SED slope. However, the typical range of infrared variability for young stars (e.g., Cohen & Schwartz 1976) is not large enough to produce most of the observed SEDs if the "true" SED from simultaneous photometry were indeed a power law. In particular, we can securely say that in three of the four binaries modeled in detail above, the observed range of variability is not enough to produce the observed deviations from power-law SED structure. Interestingly AK Sco, which is the most photometrically variable of the four [Fig. 4(a)], has an SED slope that *is* nearly a power law.

Another possible source of uncertainty in the SEDs is extended emission in the *IRAS* beam. For some of the single stars, the only measurements available at $\lambda > 3$ μm are from *IRAS*, and thus determination of the SED slopes depends heavily on the *IRAS* data. Because of the differing beam sizes of the *IRAS* observations compared to typical ground-based infrared observations, the *IRAS* fluxes may be higher due to contributions from emission on scales of $10''$–$60''$ (Young et al. 1986). One constraint on the presence of extended emission is a comparison of ground-based N and Q (10.1 and 20 μm) fluxes, typically made with beam sizes of order $5''$, with *IRAS* 12 and 25 μm fluxes, which had beam sizes of roughly $45''$ (Weaver & Jones 1992). For three of the four binaries in our main sample, these fluxes agree reasonably well or the ground-based flux is higher (Figs. 1–4), indicating that most of the 12 and 25 μm emission comes from size scales of $5''$ or less (i.e. within roughly 350 AU of the binary). Only V4046 Sgr has *IRAS* fluxes that are higher than the ground-based fluxes, but its SED still shows clear evidence of a hole when only the ground-based data are used. Thus, extended emission on larger scales cannot account for the observed SED structure of the binaries. Among the single stars, 8 of 13 have both N and *IRAS* 12 μm measurements; in most cases they agree reasonably well. Thus, while extended emission may be a factor for some of the single star SEDs, it is not a dominant contributor to the emission for the majority of systems.

Boss & Yorke (1993, 1996) calculated disk models that take into account expected dust opacity changes due to grain evaporation and condensation in the region of the disk from 1–10 AU. They found that such a model can produce small dips in the infrared SEDs of continuous disks; such opacity changes are a possible explanation for some of the observed SED structure. Indeed, it is unlikely that the simple model discussed here describes well the true complexity of accretion disks, and it is quite possible that disks have more complicated temperature and opacity distributions. However, we also emphasize that opacity and temperature changes of this type *cannot* reproduce the observed SEDs of V4046 or 162814−2427, nor those of the three single stars with similar SEDs.

None of the effects discussed above can reproduce the observed diversity of SEDs. Thus, it is possible that the observed deviations from power-law SEDs among some of the single stars do indeed reflect the presence of gaps in their disks. Several authors have noted that the absence of near-infrared excesses in some single T Tauri stars suggests the presence of central holes (Strom et al. 1989, BSCG, Marsh & Mahoney 1992, Koerner et al. 1993); we concur that in at least three cases, stars that are apparently single seem to have central holes in their disks. Given this fact, we cannot categorically conclude that the holes in the disks of 162814−2427 and V4046 Sgr must have been cleared because they are binaries. The holes in the disks of single stars have been interpreted as possibly due to planetesimal accumulation (Strom et al. 1989), a process that could occur in the binary systems as well.

However, the excellent agreement between dynamical predictions and observations for the size scale of the clearing in the binary systems studied above is compelling evidence that the binary companion has played a role in establishing the cleared regions.

SED structures consistent with gaps or holes in disks have also been interpreted as indicative of the presence of unseen companions, perhaps with substellar masses (Marsh & Mahoney 1992, 1993). We note that our finding above that several binaries with known stellar companions *do not* show "unusual" SEDs suggests that the lack of any apparent structure in the SED of a young star does not necessarily rule out the presence of a planetary companion.

6. Summary and Conclusions

We have compiled spectral energy distributions from optical to millimeter wavelengths for four low-mass pre–main-sequence spectroscopic binaries. These binaries all have infrared excesses, presumed to be evidence for associated disks. If these binaries clear gaps or holes in their disks on size scales comparable to their semi-major axes ($a \lesssim 1$ AU), then their SEDs should be characterized by a relative deficit of emission at wavelengths between roughly 1 μm and 10 μm.

Three of these binaries (162814−2427, V4046 Sgr, and 162819−2423S) show small or no near-infrared excess emission but large excess emission at wavelengths of 10 μm and longer. These SEDs suggest that the binaries reside within optically thin regions surrounded by optically thick circumbinary disks. Comparisons with theoretical SEDs show that the observed SEDs are consistent with cleared gaps or holes having the dimensions predicted by dynamical theory.

On the other hand, the fourth binary (AK Sco) shows a continuous power-law SED from 1–60 μm, surprising if the binary has cleared a region out to 0.5 AU as predicted by dynamical theory. Evidently this system contains extended material having a distribution of temperature between photospheric and circumbinary disk temperatures, suggesting the presence of material in the region expected to be dynamically cleared. Similar SEDs have been seen from the pre–main-sequence binaries DQ Tau and UZ Tau E.

Such power-law SEDs do not indicate dynamically cleared regions. Nonetheless, dynamical clearing is not precluded; the only secure conclusion is that the inner regions are not cleared completely. Indeed, a strong silicate emission feature from AK Sco suggests the presence of hot optically thin dust, possibly in a dynamically cleared region. We have successfully modeled the SED of AK Sco, including the silicate emission, with a dynamically cleared hole in which a very small amount ($\sim 10^{-9}\ M_\odot$) of isothermal material is present. This particular model is too simple to be physically accurate, but it nonetheless makes the point that very little hot dust is required to produce the observed near-infrared excess and silicate emission feature.

Most of these pre–main–sequence spectroscopic binaries show some near-infrared excess, implying the presence of hot material near the stars. This is significant given that the dynamical constraints on the radii of circumstellar disks are in many cases less than 0.1 AU. Consequently the distribution of this material is very uncertain and indeed may not be disk-like. Its source is also unclear, but it must be replenished since either viscosity in circumstellar disks or Poynting-Robertson drag on optically thin material would move such material onto the stars on short timescales. Perhaps the material flows from the circumbinary disks, for example in the accretion streams recently suggested by Artymowicz & Lubow (1996) or due to the Poynting-Robertson effect on the inner edge of the circumbinary disks.

All of the binaries studied here have circumbinary disks, with masses ranging from 0.06 $M_\odot$ to less than $10^{-4}\ M_\odot$. The larger disk masses are sufficient to change the binaries' orbital eccentricities substantially during their PMS lifetimes.

To close, we have found that short-period pre–main-sequence spectroscopic binaries show a broad range of SED structures; evidently the spatial distribution of disk material is more complex than in simple dynamical-clearing models. Nonetheless the SEDs are consistent with binaries clearing regions in associated disks on size scales comparable to orbital separations, although these regions may not be entirely evacuated. Circumstellar material is typically present, perhaps replenished from circumbinary disks and providing a source for continued accretion onto the stars. Interestingly, single stars show a similar diversity of SED structures, with several having SEDs very similar to those of the binaries 162814−2427, 162819−2423S, and V4046 Sgr. Presuming that clearing by the stellar companions is the origin of the SED structures of the close binaries, the implication is that the disks of the single stars have also been cleared.

We thank F. Vrba for sharing observations of 162819−2423S. We thank the staffs of the IRTF and UKIRT for assistance with the observations reported here, in particular K. Krisciunas for assistance with UKIRT data reduction. F. Adams provided the foundation for our disk modeling, and W. Caplan assisted in our initial explorations. We are very appreciative of many valuable discussions on binary-disk interactions, especially with P. Artymowicz, P. Cassen, D. Lin and S. Lubow. The comments of the referee were very helpful. ELNJ gratefully acknowledges the support of the National Space Grant College and Fellowship Program and the Wisconsin Space Grant Consortium. RDM appreciates funding from the Presidential Young Investigator program, the Wisconsin Alumni Research Fund, and NSF grant AST-9417195.

Table 1. Orbital data for PMS binaries with disks and $a \lesssim 1$ AU

Name	$a \sin i$ (AU)	Period (Days)	Eccentricity	Location
V4046 Sgr	0.024	2.4	0	Isolated
W134	0.099	6.353	0	NGC 2264
AK Sco	0.143	13.6	0.47	Upper Sco
DQ Tau	0.053	15.8	0.58	Taurus-Auriga
UZ Tau E	0.03	19.1	0.28	Taurus-Auriga
162814−2427	0.267	40.0	0.48	ρ Oph
V773 Tau	0.34	51.075	0.267	Taurus-Auriga
162819−2423S	0.10	89.1	0.41	ρ Oph
GW Ori	0.10	241.9	0.04	Orion

Table 2. IRTF broad-band photometry

Star	J	H	K	L'	M	N	Q	Notes
155808−2219	⋯	⋯	⋯	⋯	7.85 ± 0.35	⋯	⋯	a
	9.67 ± 0.03	8.90 ± 0.03	8.68 ± 0.01	8.46 ± 0.09	⋯	⋯	⋯	b
155913−2233	⋯	⋯	⋯	⋯	⋯	7.75 ± 1.28	⋯	d
162218−2420	⋯	⋯	⋯	⋯	7.53 ± 0.15	⋯	⋯	c
	⋯	⋯	⋯	⋯	7.58 ± 0.16	7.91 ± 1.33	⋯	d
162814−2427	⋯	⋯	⋯	⋯	6.62 ± 0.05	⋯	⋯	a
	8.32 ± 0.02	7.41 ± 0.02	7.12 ± 0.01	6.58 ± 0.05	6.47 ± 0.09	⋯	⋯	b
	⋯	⋯	7.13 ± 0.03	⋯	⋯	4.98 ± 0.11	2.60 ± 0.21	c
162819−2423N	⋯	⋯	7.68 ± 0.10	⋯	7.07 ± 0.13	5.73 ± 0.16	⋯	d
162819−2423S	⋯	⋯	⋯	⋯	5.61 ± 0.03	3.25 ± 0.03	⋯	a
	7.98 ± 0.02	7.20 ± 0.02	6.74 ± 0.01	5.95 ± 0.05	5.66 ± 0.11	⋯	⋯	b
	⋯	⋯	6.96 ± 0.03	⋯	⋯	3.14 ± 0.03	1.71 ± 0.18	c
	⋯	⋯	6.89 ± 0.10	⋯	5.84 ± 0.10	⋯	⋯	d
AK Sco	⋯	⋯	⋯	⋯	5.11 ± 0.04	2.83 ± 0.03	0.85 ± 0.07	a
	7.46 ± 0.03	6.83 ± 0.03	6.18 ± 0.01	5.01 ± 0.09	4.35 ± 0.11	⋯	⋯	b
AS 205	⋯	⋯	5.60 ± 0.03	⋯	⋯	1.73 ± 0.01	0.01 ± 0.12	c
FK Ser	⋯	⋯	6.61 ± 0.01	⋯	5.90 ± 0.06	4.42 ± 0.09	2.58 ± 0.17	d
Haro 1-4	⋯	⋯	7.64 ± 0.04	⋯	⋯	4.57 ± 0.08	2.50 ± 0.22	c
SR 20	⋯	⋯	⋯	⋯	⋯	6.07 ± 0.34	⋯	c

Table 2—Continued

Star	J	H	K	L'	M	N	Q	Notes
V4046 Sgr	$\cdots$	$\cdots$	$\cdots$	$\cdots$	7.30 ± 0.07	$\cdots$	$\cdots$	a
	7.93 ± 0.03	7.29 ± 0.03	7.18 ± 0.01	7.04 ± 0.09	7.28 ± 0.17	$\cdots$	$\cdots$	b
	$\cdots$	$\cdots$	7.28 ± 0.03	$\cdots$	$\cdots$	5.39 ± 0.11	2.51 ± 0.30	c
	$\cdots$	$\cdots$	$\cdots$	$\cdots$	$\cdots$	5.21 ± 0.10	2.95 ± 0.57	d
V853 Oph	$\cdots$	$\cdots$	7.97 ± 0.04	$\cdots$	$\cdots$	4.58 ± 0.06	3.48 ± 1.06	c
WL 22	$\cdots$	$\cdots$	7.52 ± 0.04	$\cdots$	4.99 ± 0.03	2.86 ± 0.02	0.93 ± 0.10	c

Note. — Observation dates (UT): (a) 9 June 1992; (b) 10 June 1992; (c) 18 June 1993; (d) 19 June 1993.

Table 3. IRTF narrow-band photometry

Star	[7.8 μm]	[8.7 μm]	[9.8 μm]	[10.3 μm]	[11.6 μm]	[12.5 μm]	Notes
162819−2423S	4.77 ± 0.10	3.70 ± 0.05	2.97 ± 0.04	2.94 ± 0.04	2.78 ± 0.04	3.08 ± 0.09	a
AK Sco	4.06 ± 0.06	2.88 ± 0.04	2.10 ± 0.03	2.12 ± 0.04	2.26 ± 0.03	2.79 ± 0.07	a
FK Ser	$\cdots$	4.88 ± 0.10	$\cdots$	4.30 ± 0.09	4.14 ± 0.14	4.21 ± 0.29	b
Haro 1-4	5.95 ± 0.38	5.06 ± 0.09	4.35 ± 0.10	4.58 ± 0.10	4.25 ± 0.13	3.98 ± 0.14	b

Note. — Observation dates (UT): (a) 9 June 1992; (b) 19 June 1993.

Table 4. UKIRT photometry, 26 May 1993

Star	J	H	K	L'	M[a]
160946−1851	8.40 ± 0.02	7.73 ± 0.02	7.56 ± 0.01	7.41 ± 0.01	7.65 ± 0.04
162814−2427	8.62 ± 0.01	7.68 ± 0.01	7.27 ± 0.01	6.70 ± 0.01	6.53 ± 0.02
162819−2423S	8.20 ± 0.01	7.51 ± 0.01	7.07 ± 0.01	6.21 ± 0.01	5.84 ± 0.01
AK Sco	7.86 ± 0.01	7.14 ± 0.01	6.41 ± 0.01	5.27 ± 0.01	4.94 ± 0.01
AS 205	7.96 ± 0.02	6.71 ± 0.02	5.74 ± 0.01	4.27 ± 0.01	3.74 ± 0.02
Haro 1-4	9.24 ± 0.01	8.20 ± 0.01	7.71 ± 0.01	6.87 ± 0.01	6.59 ± 0.03
SR 12	9.43 ± 0.01	8.69 ± 0.01	8.45 ± 0.01	8.18 ± 0.02	8.27 ± 0.07
SR 20	8.86 ± 0.01	7.71 ± 0.01	7.19 ± 0.01	6.79 ± 0.01	6.77 ± 0.02
SR 21	8.75 ± 0.01	7.42 ± 0.01	6.40 ± 0.01	4.97 ± 0.01	4.61 ± 0.01
SR 24N	10.78 ± 0.01	9.23 ± 0.01	8.21 ± 0.01	6.75 ± 0.01	6.21 ± 0.02
SR 24S	9.85 ± 0.01	8.39 ± 0.01	7.41 ± 0.01	6.14 ± 0.01	5.70 ± 0.01
SR 4	9.18 ± 0.02	8.17 ± 0.01	7.53 ± 0.01	6.49 ± 0.01	6.10 ± 0.01
SR 9	8.58 ± 0.01	7.73 ± 0.01	7.21 ± 0.01	6.36 ± 0.01	6.13 ± 0.02
V4046 Sgr	8.14 ± 0.01	7.51 ± 0.01	7.37 ± 0.01	7.17 ± 0.01	7.17 ± 0.03
V853 Oph	9.18 ± 0.01	8.38 ± 0.01	7.83 ± 0.01	6.88 ± 0.01	6.48 ± 0.02

[a]These observations used the UKIRT narrow-band M filter ($\lambda = 4.64$ μm, $\Delta\lambda = 0.175$ μm FWHM). Narrow-band M magnitudes should be within a few percent of magnitudes measured in the standard M filter (Geballe 1992).

Table 5. Adopted parameters for PMS binaries

HBC[a]	Name	Alternate name	Spectral type	Inclin- ation	A_V	$r_{\rm in}$ (AU)	$r_{\rm out}$ (AU)
···	162814−2427	ROXs 42C	K4[b]	71° [c]	1.6[b]	0.057	0.85
662	V4046 Sgr	HD 319139	K5[d]	37° [d]	0[c]	0.016	0.072
···	162819−2423S	ROXs 43A	G0[e]	60° [c]	2.4[c]	0.023	0.35
271	AK Sco	HD 152404	F5[f]	63° [f]	0.4[f]	0.032	0.48

[a]Number from the catalog of Herbig & Bell (1988).

[b]Lee (1992).

[c]This work; see text.

[d]de la Reza et al. (1986).

[e]Walter et al. (1994).

[f]Andersen et al. (1989).

Table 6. Optical photometry of ρ Oph binaries

Star	U	B	V	R_C	I_C
162814−2427[a]	14.805	13.505	11.92	10.90	9.93
162819−2423S[b]	12.99	12.04	10.86	10.14	9.39
162819−2423N[b]	13.46	13.47	12.18	11.26	10.36

[a]Observations made 26 May 1989 (UT) by Dr. Harry Guetter, USNO, as quoted in Lee (1992).

[b]Observations made 6 July 1993 (UT) by Dr. Fred Vrba, USNO. The magnitudes given are from combined-light observations of 162819−2423S and 162819−2423N made with a 15″ aperture, which were split using flux ratios measured in a 5″ aperture. All measurements have approximately 0.02 magnitude uncertainty.

Table 7. Disk masses

Name	Disk mass ($10^{-3}\ M_{\odot}$)
V4046 Sgr	8.5
AK Sco	1.7
DQ Tau	20.[a]
UZ Tau E	63.[b]
162814−2427	< 0.25
162819−2423S	< 0.37
GW Ori	300.[c]

[a]Mathieu et al. (1997).

[b]Jensen et al. (1996b).

[c]Mathieu et al. (1995).

REFERENCES

Adams, F. C., Emerson, J. P., & Fuller, G. A. 1990, ApJ, 357, 606

Adams, F. C., Lada, C. J., & Shu, F. H. 1988, ApJ, 326, 865 (ALS88)

Agladze, N. I., Sievers, A. J., Jones, S. A., Burlitch, J. M., & Beckwith, S. V. W. 1994, Nature, 372, 243

Agladze, N. I., Sievers, A. J., Jones, S. A., Burlitch, J. M., & Beckwith, S. V. W. 1996, ApJ, 426, 1026

Andersen, J., Lindgren, H., Hazen, M. L., & Mayor, M. 1989, A&A, 219, 142

Artymowicz, P., Clarke, C. J., Lubow, S. H., & Pringle, J. E. 1991, ApJ, 370, L35

Artymowicz, P., & Lubow, S. H. 1994, ApJ, 421, 651

Artymowicz, P., & Lubow, S. H. 1996, ApJ, 467, L77

Basri, G., Johns-Krull, C., & Mathieu, R.D. 1997, AJ, submitted

Beckwith, S. V. W., & Sargent, A. I. 1991, ApJ, 381, 250

Beckwith, S. V. W., Sargent, A. I., Chini, R. S., & Güsten, R. 1990, AJ, 99, 924 (BSCG)

Boss, A. P., & Yorke, H. W. 1993, ApJ, 411, L99

Boss, A. P., & Yorke, H. W. 1996, ApJ, 469, 366

Bouvier, J., & Appenzeller, I. 1992, A&A, 92, 481

Buser, R., & Kurucz, R. L. 1992, A&A, 264, 557

Busko, I. C., & Torres, C. A. O. 1976, IBVS, 1186

Busko, I. C., & Torres, C. A. O. 1978, A&A, 64, 153

Byrne, P. B. 1986, Irish Astron. J., 17, 294

Cardelli, J. A., Clayton, G. C., & Mathis, J. S. 1989, ApJ, 345, 245

Clark, F. O. 1991, ApJS, 75, 611

Cohen, M. 1974, MNRAS, 169, 262

Cohen, M., & Schwartz, R. D. 1976, MNRAS, 174, 137

Cohen, M., & Witteborn, F. C. 1985, ApJ, 294, 345

D'Antona, F., & Mazzitelli, I. 1994, ApJS, 90,467

de Geus, E. J., de Zeeuw, P. T., & Lub, J. 1989, A&A, 216, 44

de la Reza, R., Quast, G., Torres, C. A. O., Mayor, M., Meylan, G., & Llorente de Andrés, F. 1986, New Insights in Astrophysics (Noordwijk: ESA), 107

Dutrey, A., Guilloteau, S., Duvert, G., Prato, L., Simon, M., Schuster, K., & Menard, F. 1996, A&A, 309, 493

Dutrey, A., Guilloteau, S., & Simon, M. 1994, A&A, 286, 149

Geballe, T. 1992, UKIRT newsletter, p. 6

Ghez, A. M., Emerson, J. P., Graham, J. R., Meixner, M., & Skinner, C. J. 1994, ApJ, 434, 707

Ghez, A. M., Neugebauer, G., & Matthews, K. 1993, AJ, 106, 2005

Gregorio-Hetem, J., Lépine, J. R. D., Quast, G. R., Torres, C. A. O., & de la Reza, R. 1992, AJ, 103, 549

Hanner, M. S., Tokunaga, A. T., Veeder, G. J., & A'Hearn, M. F. 1984, AJ, 89, 162

Henning, T., & Stognienko, R. 1996, A&A, 311, 291

Herbig, G. H., & Bell, K. R. 1988, Lick Observatory Bulletin 1111

Herbst, W., Herbst, D. K., Grossman, E. J., & Weinstein D. 1994, AJ, 108, 1906

Hildebrand, R. H. 1983, QJRAS, 24, 267

Hutchinson, M. G., Barrett, P., Davies, J. K., Evans, A., Goldsmith, M. J., & Maddison, R. C. 1994, A&A, 285, 883

Hutchinson, M. G., Evans, A., Winkler, H., & Spencer Jones, J. 1990, A&A, 234, 230

Jäger, C., Mutschke, H., Begemann, B., Dorschner, J., & Henning, Th. 1994, A&A, 292, 641

Jensen, E. L. N., Koerner, D. W., & Mathieu, R. D. 1996b, AJ, 111, 2431

Jensen, E. L. N., Mathieu, R. D., & Fuller, G. A. 1994, ApJ, 429, L29

Jensen, E. L. N., Mathieu, R. D., & Fuller, G. A. 1996a, ApJ, 458, 312

Kenyon, S. J., & Hartmann, L. 1995, ApJS, 101, 117

Kilkenny, D., Whittet, D. C. B., Davies, J. K., Evans, A., Bode, M. F., Robson, E. I., & Banfield, R. M. 1985, South African Astron. Obs. Circ., 9, 55

Koerner, D. W., Sargent, A. I., & Beckwith, S. V. W. 1993, ApJ, 408, L93

Königl, A. 1991, ApJ, 370, L39

Krügel, E., & Siebenmorgen, R. 1994, A&A, 288, 929

Lang, K. R. 1992, Astrophysical Data: Planets and Stars (New York:Springer-Verlag), 138

Lee, C. W. 1992, Ph.D. thesis, University of Wisconsin-Madison

Lee, C. W. 1994, private communication

Leinert, Ch., Zinnecker, H., Weitzel, N., Christou, J., Ridgway, S., Jameson, R., Haas, M., & Lenzen, R. 1993, A&A, 278, 129

Lin, D. N. C., & Papaloizou, J. 1993, in Protostars and Planets III, ed. E. H. Levy & J. I. Lunine (Tucson:University of Arizona Press), 749

Lubow, S. H., & Artymowicz, P. 1992, in Binaries as Tracers of Stellar Formation, ed. A. Duquennoy & M. Mayor (Cambridge: Cambridge University Press), 145

Lubow, S. H., & Artymowicz, P. 1996, in Evolutionary Processes in Binary Stars, ed. R. A. M. J. Wijers, M. B. Davies, & C. A. Tout (Dordrecht: Kluwer Academic Publishers), 53

Marsh, K. A., & Mahoney, M. J. 1992, ApJ, 395, L115

Marsh, K. A., & Mahoney, M. J. 1993, ApJ, 405, L71

Mathieu, R. D. 1994, ARA&A, 32, 465

Mathieu, R. D., Adams, F. C., Fuller, G.A., Jensen, E. L. N., Koerner, D. W., & Sargent, A. I. 1995, AJ, 109, 2655

Mathieu, R. D., Adams, F. C., & Latham, D. W. 1991, AJ, 101, 2184

Mathieu, R. D., Martín, E. L., & Maguzzu, A. 1996, BAAS, 28, 920

Mathieu, R. D., Stassun, K., Basri, G., Johns-Krull, C., Jensen, E. L. N., & Hartmann, L. 1997, AJ, in press

Mathieu, R. D., Walter, F. M., & Myers, P. C. 1989, AJ, 98, 987

Osterloh, M., & Beckwith, S. V. W. 1995, ApJ, 439, 288

Padgett, D. L. and Stapelfeldt, K. R., 1994, AJ, 107, 720

Pollack, J. B., Hollenbach, D., Beckwith, S., Simonelli, D. P., Roush, T., & Fong, W. 1994, ApJ, 421, 615

Press, W. H., Teukolsky, S. A., Vetterling, W. T., & Flannery, B. P. 1992, Numerical Recipes in FORTRAN: The Art of Scientific Computing (New York: Cambridge University Press), 678

Reipurth, B., & Zinnecker, H. 1993, A&A, 278, 81

Roddier, C., Roddier, F., Northcott, M. J., Graves, J. E., & Jim, K. 1996, ApJ, 463, 326

Rucinski, S. M., & Krautter, J. 1983, A&A, 121, 217

Sargent, A. I. 1996, in Disks and Outflows Around Young Stars, ed. Beckwith, S. V. W., Natta, A., & Staude, H. J. (Berlin: Springer-Verlag), 1

Shu, F., Najita, J., Ostriker, E., Wilkin, F., Ruden, S., & Lizano, S. 1994, ApJ, 429, 781

Simon, M., Ghez, A. M., & Leinert, Ch. 1993, ApJ, 408, L33

Simon, M., Ghez, A. M., Leinert, Ch., Cassar, L., Chen, W. P., Howell, R. R., Jameson, R. F., Matthews, K., Neugebauer, G., & Richichi, A. 1995, ApJ, 443, 625

Simon, M., & Prato, L. 1995, ApJ, 450, 824

Strom, K. M., Strom, S. E., Edwards, S., Cabrit, S., & Skrutskie, M. F. 1989, AJ, 97, 1451

Tokunaga, A. 1988, The Infrared Telescope Facility Photometry Manual

Tokunaga, A. T., Golisch, W. F., Griep, D. M., Kaminski, C. D., & Hanner, M. S. 1986, AJ, 92, 1183

Walter, F. M., Vrba, F. J., Mathieu, R. D., Brown, A., & Myers, P. C. 1994, AJ, 107, 692

Weaver, W. B., & Jones, G. 1992, ApJS, 78, 239

Welty, A. D. 1995, AJ, 110, 776

Young, E. T., Lada, C. J., & Wilking, B. A. 1986, ApJ, 304, L45

Zakirov, M. M., Azimov, A. A., & Grankin, K. N. 1993, IBVS, 3898

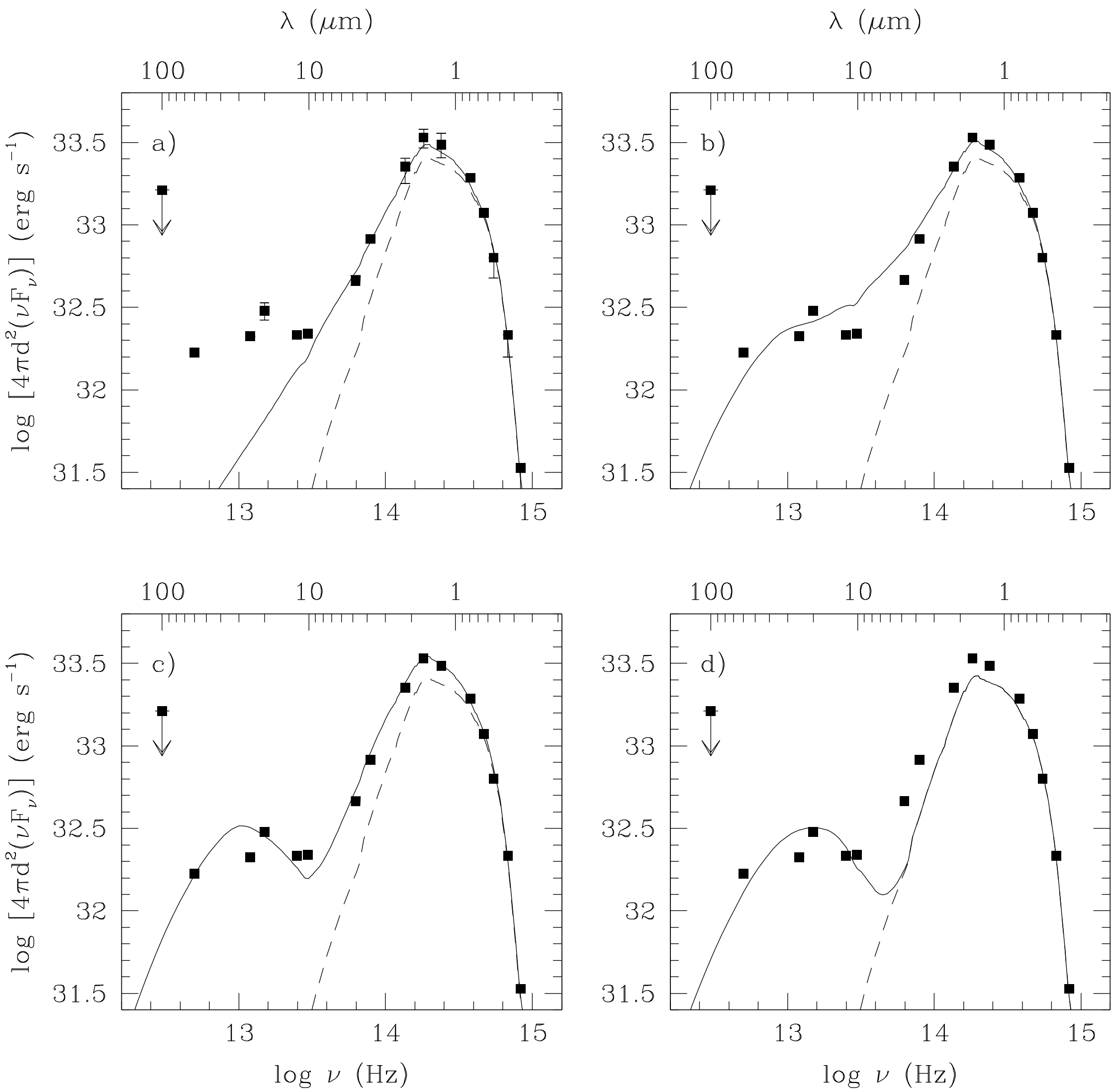

Fig. 1.— Disk models of the 162814−2427 system. The dashed line shows the contribution from the stellar photospheres, and the solid line shows the total star+disk emission. (a) A continuous reprocessing disk; the error bars show the observed range of variability at each wavelength. (b) A continuous "active" disk, *i.e.* a disk with a flatter temperature distribution. (c) A disk with the dynamically predicted gap size of $r_{\rm in} = 0.057$ AU and $r_{\rm out} = 0.85$ AU. (d) A disk with an inner hole out to $r_{\rm out} = 0.85$ AU. The model with a gap provides a much better fit to the data than either of the continuous disk models.

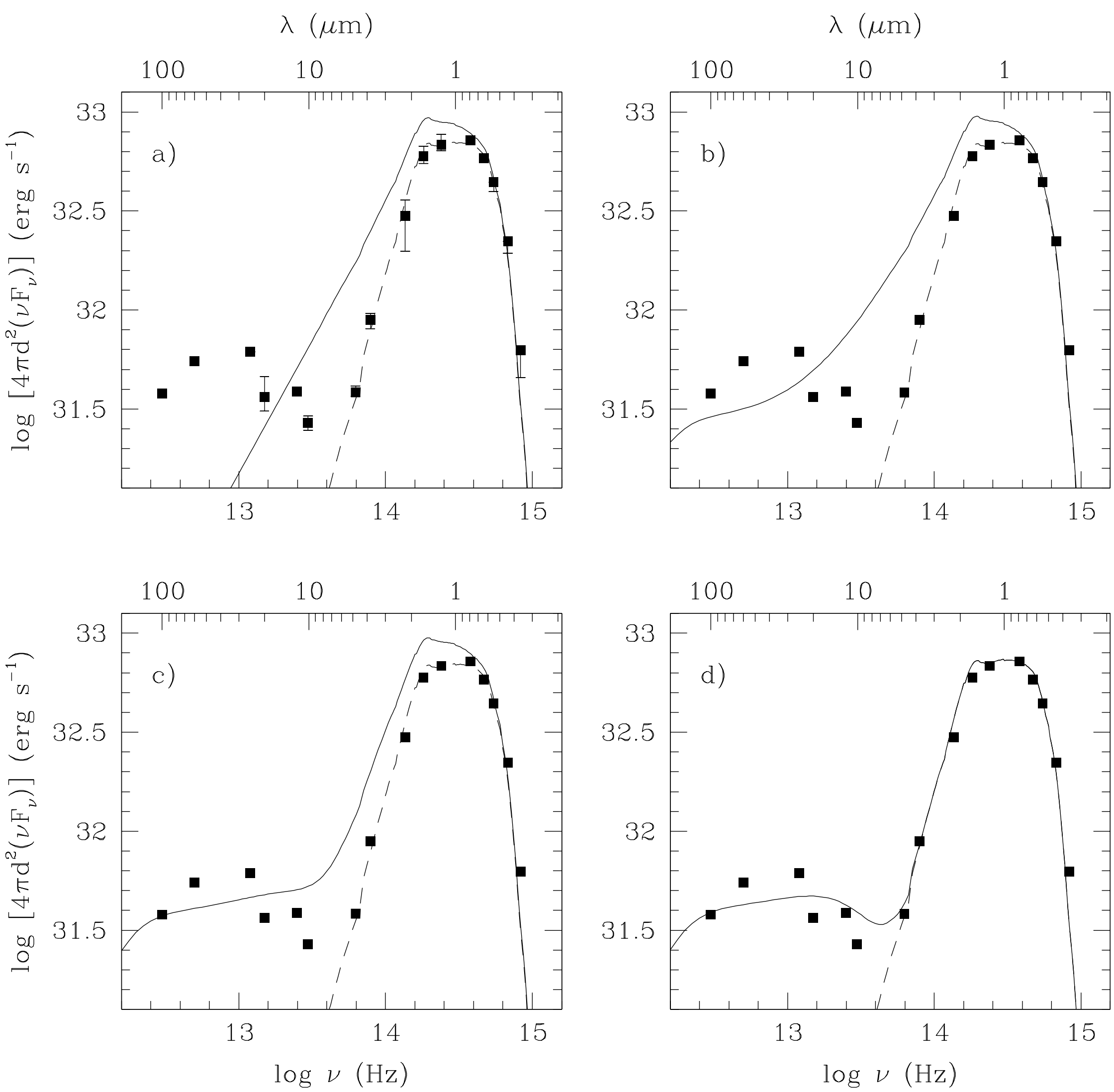

Fig. 2.— Disk models of the V4046 Sgr system, as in Fig. 1. (a) A continuous reprocessing disk. The data fall below the model between 1 and 5 μm, indicating that the regions of the disk that dominate the emission at these wavelengths are optically thin. (b) A continuous active disk. (c) A disk with the dynamically predicted gap size of $r_{\rm in}$ = 0.016 AU and $r_{\rm out}$ = 0.072 AU. (d) A disk with an inner hole out to $r_{\rm out}$ = 0.072 AU. The hole model provides the best fit to the data.

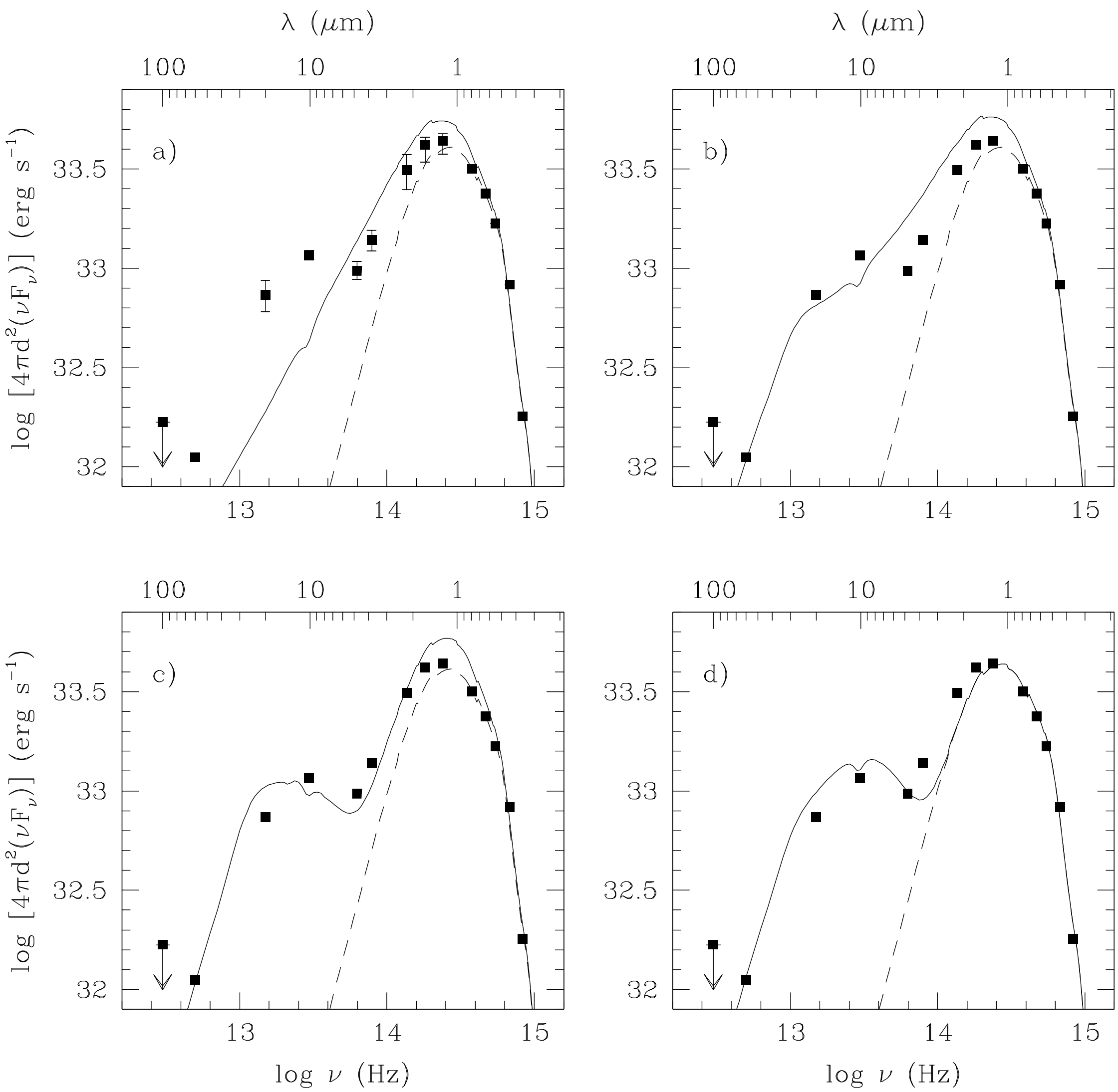

Fig. 3.— Disk models of the 162819−2423S system, as in Fig. 1. (a) A continuous reprocessing disk. (b) A continuous active disk. (c) A disk with the dynamically predicted gap size of $r_{\rm in} = 0.023$ AU and $r_{\rm out} = 0.35$ AU. (d) A disk with an inner hole out to $r_{\rm out} = 0.35$ AU. The dynamic gap and hole models provide the best fits to the data, reproducing the change in spectral slope around 5 μm.

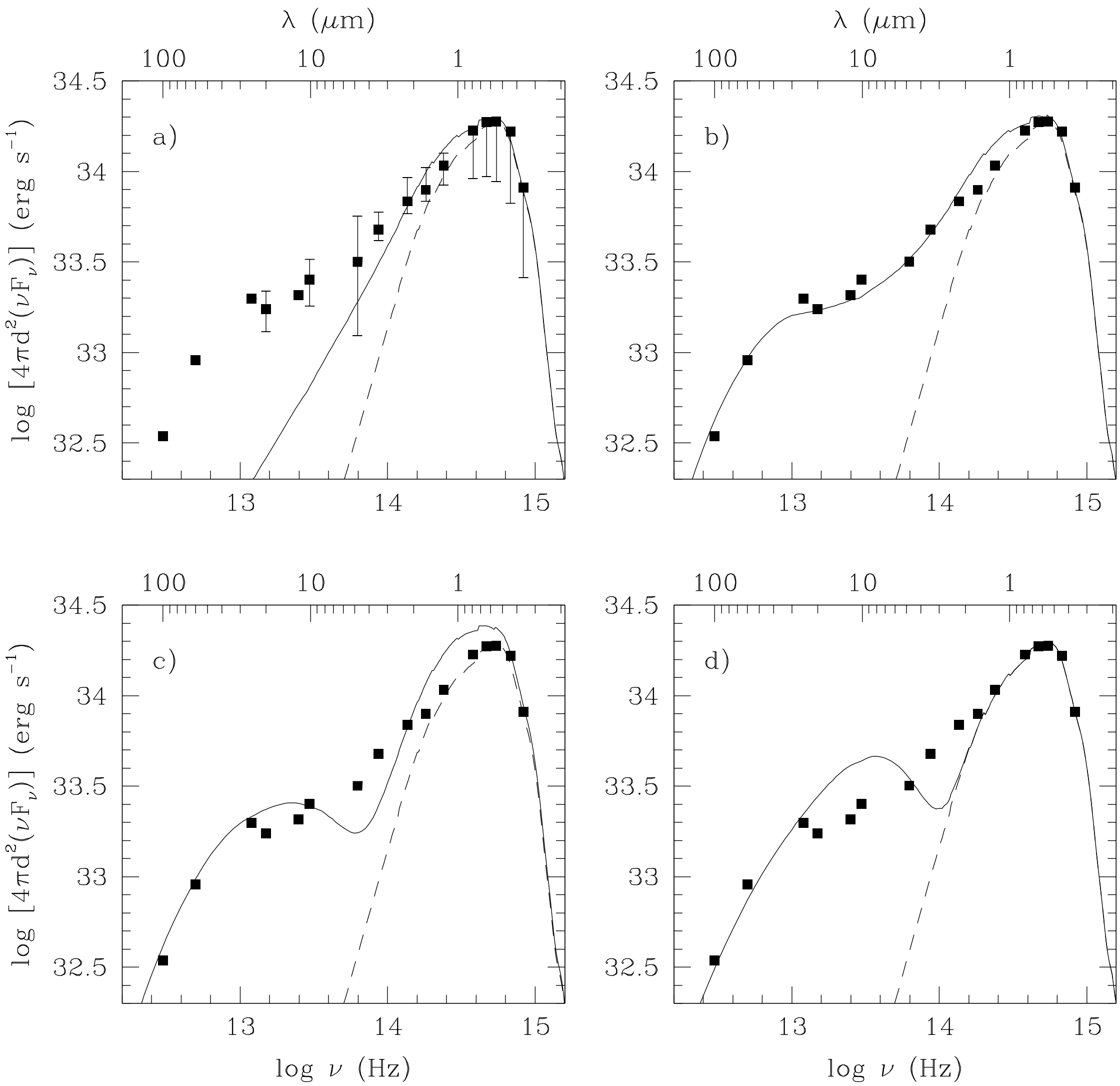

Fig. 4.— Disk models of the AK Sco system, as in Fig. 1. (a) A continuous reprocessing disk. The data fall slightly below the model at 1–2 μm, hinting at an optically thin inner disk. (b) A continuous active disk. (c) A disk with the dynamically predicted gap size of $r_{\rm in} = 0.032$ AU and $r_{\rm out} = 0.48$ AU. (d) A disk with an inner hole out to $r_{\rm out} = 0.48$ AU. Unlike the other systems, the continuous active disk provides the best fit to the broad-band SED.

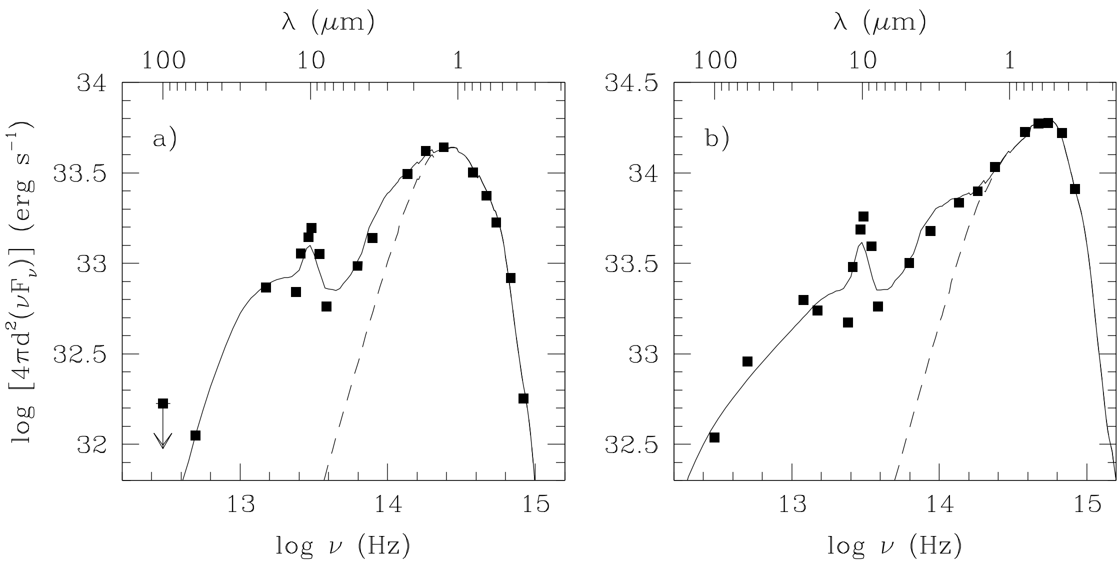

Fig. 5.— Disk models of the 162819−2423S and AK Sco systems with an optically thin dust component ($T_{\rm dust} = 1000$ K) added to fit the silicate emission feature. (a) 162819−2423S with the dynamically predicted hole (see Fig. 3) and $\tau_{10\,\mu{\rm m}} = 0.2$ for the added dust component. (b) AK Sco with the dynamically predicted hole (see Fig. 4) and $\tau_{10\,\mu{\rm m}} = 0.4$. The SEDs of both systems are consistent with cleared (but not entirely evacuated) regions in their disks; the mass of optically thin material is $\sim 10^{-9}\ M_\odot$.